September 21, 2015

MASTER THESIS

APPLICATION OF RAPID PROTOTYPING IN TRAUMA SURGERY: CLAVICLE FRACTURE REPAIR - A CLINICAL STUDY

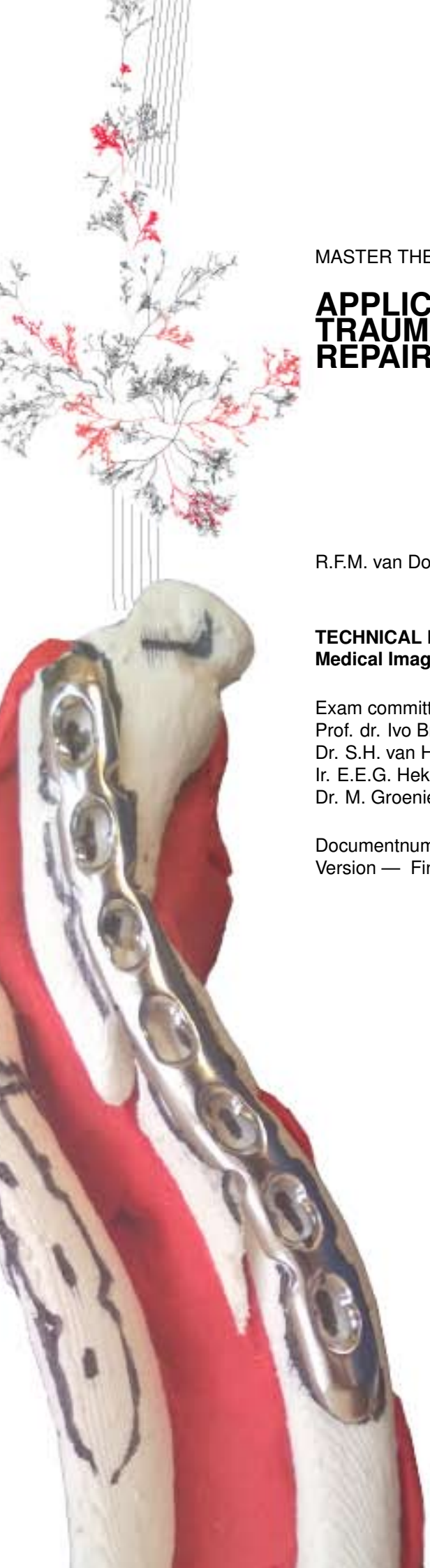

R.F.M. van Doremalen

TECHNICAL MEDICINE
Medical Imaging and Intervention

Exam committee:
Prof. dr. Ivo Broeders – chairman
Dr. S.H. van Helden – medical
Ir. E.E.G. Hekman – technical
Dr. M. Groenier – process

Documentnumber
Version — Final

UNIVERSITY OF TWENTE.

Summary

Introduction: This research focusses on surgical fracture treatment in trauma surgery. One method to operatively fix a fracture is open reduction and internal fixation by means of plates and screws. In case of fractures in bones with complex shapes, the plate seldom fits. The aim of this thesis was to create and test a method to preoperatively obtain a fitting osteosynthesis plate. The hypothesis was that this would result in shorter plate handling time and improvement in surgical workflow.
Methods: A prospective controlled intervention trial was performed with patients that presented with a clavicle fracture. In the intervention group two three-dimensional (3D) plastic bone models were created by using consecutive CT imaging, segmentation, volume rendering and were subsequently fabricated by means of rapid prototyping. The first model is a replica of the fractured bone and the second a reconstruction created by mirroring the contralateral bone. A standard osteosynthesis plate could then be preoperatively bent according to these models to be used during the scheduled surgery. This method was validated by performing a bone and phantom validation study to find the lowest applicable radiation dose.
The control group consisted of patients with clavicle fractures. All were treated with standard plates that had to be adjusted during the surgery.
Results: Eight subjects were included in the control group and seven in the intervention group. A plate handling time reduction of 2:04 minutes (p:0.563) was measured, however, there was a lengthened surgery time of 9:22 minutes (p:0.132). A good integration of the method in the workflow was accomplished, but measurements were subjective and inconclusive. The bone validation study resulted in an acceptance of an average distance deviation of 1.04 mm, acquired with half the dose.
Conclusion: It is possible to integrate rapid prototyping in trauma surgery to preoperatively create fitting osteosynthesis plates. However, in case of clavicle fractures, the extra effort and dosage from the CT-scan do not outweigh the benefits. This method may prove its additional value in more complex fracture types.

Contents

Chapter 1

Introduction

In trauma surgery one of the primary occupations is fracture treatment. Fracture treatment can be performed closed, by means of a splint, cast, sling or external fixator, or open. Open fracture treatment means surgical reduction and fixation. The main surgical options are an intramedullary rod or open reduction and internal fixation (ORIF) by means of osteosynthesis plate and screws.

In case of a fracture in bones with a curved shape, precontoured plates are available or standard reconstruction plates can be used. The reconstruction plates need to be perioperatively bent. Even with precontoured plates, perioperative bending is required in some cases, which is undesirable. This report describes the clinical evaluation of a newly developed method to ensure a fitting plate perioperatively.

The primary surgeon, S.H. Van Helden, MD, proposed to bend the plate preoperatively based on a 3D printed replica of the fracture for clavicle fracture cases. The resulting method involved fabricating a replica of the patient's clavicle by imaging the clavicle with a CT, converting the slices into a 3D model, and subsequently 3D printing this model, also known as computer aided design and computer aided manufacturing (CAD/CAM). The replica is then used to fit an osteosynthesis plate after which this plate is sterilized for implantation. In this manner, a custom patient specific plate is available perioperatively. The method was successfully tested in a pilot pseudarthrosis case during the M2 internship, submitted and accepted as case report (appendix A).

The next objective was to investigate the feasibility of this method in general fracture treatment. More cases were needed for sufficient data and therefore a clinical study was proposed as proof of concept. The clavicle was retained as subject of this study, because of the gained experience, a relatively constant prevalence, the fact that in most cases the precontoured plate has to be bent due to the complex shape, and the fact that the possible complications are minor and in small numbers, which creates a relatively safe environment for a proof of concept. The outcome measurements were surgical time reduction and improved workflow. This clinical study came to be known as the ClaRP trail and is further discussed in chapter 4.

This thesis will first provide some background information will be provided followed by the method in detail in combination with a study to validate the method. Subsequently, the clinical study, the ClaRP trial, will be described in form of the submitted article. The thesis will end with a brief discussion and conclusion.

Chapter 2

Background

Before continuing to the main topic of this thesis, some background information will be given for support, starting with an overview of documented cases of rapid prototyping applications in literature. Subsequently, the subjects used in the method are discussed one at a time. The subjects are chronologically organized by the steps taken in the method. The first step is volumetric image acquisition by means of one of the medical imaging modalities described in ”Imaging”. Second, the images are processed into 3D models in ”Virtual Processing”. The last section describes the different relevant rapid prototyping techniques in ”Rapid prototyping”. How it all comes together in the method is described in the next chapter (3).

2.1 Applications of Rapid Prototyping in Surgery

Although most rapid prototyping techniques themselves are rather old, documentation of applications of rapid prototyping in healthcare have appeared since the beginning of the millennium. The available literature is pretty dispersed over the world. The broad alternative nomenclatures for rapid prototyping, like 3D printing and additive fabrication, creates a messy overview and difficult comparison. In the search the focus was placed on trauma and orthopaedics and on applications, instead of research models and education. Furthermore, additive manufacturing, 3D printing with tissue, was kept out of scope. In this section a short overview of varying applications in the medical field is stated. The overview is divided into developments on a global and a national level, in the Netherlands . In appendix B a tabular overview is presented of the foreign literature.

2.1.1 Global

Reports of rapid prototyping in trauma are dispersed over the world. Most of them are theoretical pieces with a couple of pilot cases. Within the reports multiple expert opinions are described that state the benefits of this method, however, quantified and objective evidence is scarce.

The more interesting articles are from Asia. Ahn et al.[1] described the process in 2006 in Korea after which, in 2014, two minimal invasive fracture treatment descriptions followed. In both articles the used pre-bent plates, one for a calcaneus fracture and the other for a clavicle fracture[2, 3]. This clavicle fracture case was the only comparable case on clavicle fracture treatment. Bagaria et al.[4] are pioneering from India and describe reduction in surgery time and a near anatomical reduction in different complex fracture type cases. The four cases described are acetabulum, calcaneal, collum, and distal femur (Hoffas) fractures. In these cases rapid prototyping was used to plan the trajectory and lengths of the screws and to pre-bent the plates. In China an interesting 3D printed external fixator is described within this topic, as well as a treatment of a thoracic spine deformity[5, 6].

Mid-America, Mexico , 2003, Brown et al.[7] were some of the first to suggest rapid prototyping as the future of trauma surgery. In North-America some more conservative articles are published. The first two were about paediatric models for better understanding and educational models of the hepatic vein for residents, which is possible under the 100 dollar[8, 9]. The last article from North-America was an objective piece about preoperative planning of hip resurfacing by introducing a patient specific femoral alignment guide during surgery[10], which was compared with navigation and the conventional wig.

The last contributing continent is Europe supplying three reviews with pilot cases, two from the UK and one from Germany[11, 12, 13], and an overview from Switzerland about the commercially available computer assisted orthopaedic surgery techniques, for instance patient specific surgical templates for arthroplasties and navigation[14].

2.1.2 Netherlands

In the Netherlands a couple of research groups and institutes are concerned with this topic. Additive manufacturing is broadly researched by the institute MIRA at the University of Twente, the MERLN Institute at Maastricht University and the orthopaedic research group at UMC Utrecht. Their area of tissue engineering intersects with rapid prototyping. In the maxillofacial reconstruction, the 3D lab in Nijmegen lead by T.J.J. Maal, PhD, uses 3D modelling for planning of, for instance, jaw reconstructions which are performed using surgical templates and custom plates[15]. They are affiliated with the mandibular surgery department of Isala, Amsterdam and Groningen[16]. From the University of Amsterdam a couple interesting articles in trauma have been published about radius malunions and a corrective osteotomy procedure using a patient-specific distal radius locking plate and surgical templates[17, 18].

2.2 Clavicle fracture

This thesis focuses on the clavicle, as mentioned in the introduction. For this reason, some deeper insight in the clavicle and the clinical aspects of a clavicle fracture is given in this section. The subject is divided in the topics anatomy and pathology, diagnosis and treatment, and epidemiology of the clavicle fracture.

2.2.1 Anatomy and pathology

The clavicle, located in the shoulder, is jointed to the sternum, the sternoclavicular (SC) joint, and to the acromion, the acromioclavicular (AC) joint. The ligaments surrounding these joints carry the equivalent name. Furthermore, the clavicle is connected to the coracoid process with the coracoclavicular ligament, connected to the first rib with the costoclavicular ligament and connected to the contralateral clavicle through the interclavicular ligament. The sternohyoid, pectoralis major and deltoid muscles find their origin on the clavicle and the sternocleidomastoid, subclavius and trapezius muscles find their insertion on the clavicle. Every limb, ligament and muscle applies force and tension on de clavicle. A schematic representation of this distribution is given in figure 2.1. Important structures such as the subclavian artery and vein, the brachial plexus and the apical segment of the lung are situated close to the clavicle[19] and therefore are prone to damage caused by the fracture or surgery.

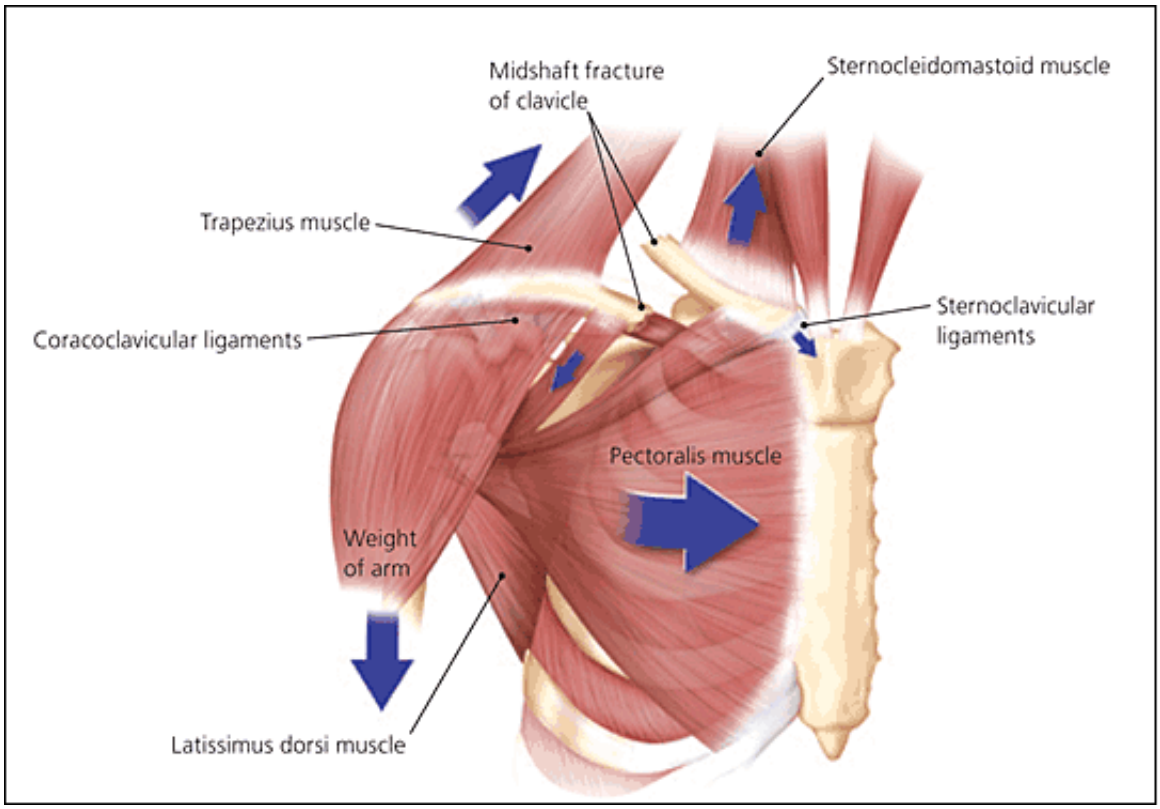

Figure 2.1: Anatomy and distributed forces after midshaft clavicle fracture. Source: www.aafp.org

We speak of a clavicle fracture, when the cortex of the bone is interrupted. There are different classifications based on the position of the fracture line(s), for example the Allman classification with Neers modification, Craig, or Robinson classification. For communication and standardization in research, the Orthopaidic Trauma Association (OTA) created an unified fracture classification in collaboration with the Arbeitsgemeinschaft fr Osteosynthesefragen (AO) for all known fractures based on existing classifications. To be able to compare this research in the literature, the OTA classification is used[20] . Clavicle fractures are divided in three sub-groups, 15-A distal fractures, 15-B midshaft fractures and 15-C proximal fractures, with additional specific sub-groups. The ClaRP trial focusses on the 15-B clavicle fractures.

The severity of a clavicle fracture can be defined by a number of factors. Initially, the fracture is assessed for complications as neurovascular compromise, open fracture, or tenting. The latter is a spike of the bone piercing against intact skin from the inside. Over time the fracture may not heal, known as nonunion, or pseudarthrosis. After six months the chance of union is slim. In some cases the fracture does heal; however, the result differs from the original anatomy and is angled or shortened, which can cause loss of function, also known as malunion. Reasons for nonunion or malunion are displacement (figure 2.1), shortening, comminution and interposed muscle or other structures.

2.2.2 Diagnosis

Clinical presentation generally consists of a patient that cradles its injured extremity with the contralateral arm. The site of fracture may seem inflamed and the shoulder may appear shortened relative to the opposite side and may droop. With gentle manipulation crepitus from the ends rubbing against each other may be noted. In more severe cases tenting and blanching of the skin at the fracture site may indicate an impending open fracture. For complete diagnosis an X-ray photo should be made of the clavicle and only in complex cases a CT scan is requested, for instance when multitrauma, multiple fractures, is suspected.

2.2.3 Treatment

The majority of these fractures are treated conservatively, with a sling. In case of tenting, open fractures, the presence of neurovascular compromise, multiple traumas or fractures with displacement and shortening, surgical treatment may be recommended[21, 22, 23, 24].

Surgical treatment entails reduction of the fracture and fixation by means of osteosynthesis material. There are roughly two choices of material. Fixation with intramedullary pen fixation or plate and screws. Plate and screw fixation, used in ORIF, is more commonly used, because the pen may lack compression at the fracture site, which can cause pin migration. Also in plate fixation hardware failure can occur, but with current precontoured clavicle locking plates the incidence is significantly reduced[25]. As in any surgical intervention, risks are involved like bleeding, neurovascular compromise and infections. Moreover, it leaves a relatively big scar. However, when the fracture is displaced surgical treatment shows better outcome on the long run than conservative treatment. Moreover, surgical treatment has a significant better functional outcome (DASH/CS, patient questionnaires), significantly lower chance of non- or malunion and a significant earlier return to daily activities and work[26, 27, 28, 29, 30, 31].

2.2.4 Epidemiology

Clavicle fractures represent 2.6% of all clinically presented adult fractures, of which the type 15-B midshaft fractures are good for 81%[21]. The local occurrence is researched in a retrospective study over the period of 2010 to October 2014 on surgical treatment of type 15-B fractures in Isala (Zwolle, the Netherlands), involving 109 subjects, table 2.1.

Table 2.1: Outcome retrospective study of surgical midshaft clavicle fracture treatment (2010-2014).

Parameter/ fracture type	Simple	Complex	total	Independent T-test sig. (2-tailed)
Amount	45 (41%)	64 (59%)	109 (100%)	
Left	21 (47%)	35 (55%)	56 (52%)	
Bent	15 (33%)	21 (33%)	36 (34%)	
Bycicle	16 (36%)	33 (52%)	49 (45%)	
2010-2013 (removed/amount)	9/37 (24%)	29/55 (53%)	38/92 (41%)	0.005
2010 (removed/amount)	3/7 (43%)	10/19 (53%)	13/26 (50%)	0.684
2011-2013 (removed/amount)	6/30 (20%)	20/36 (53%)	26/67 (39%)	0.005
T-test sig. (2010 vs 2011-2013)	0.320	0.992	0.305	

According to the surgery reports the used plate did not fit the fractured clavicle in 37 cases (34%), which is high considering only a few surgeons actually report it. These plates had to be bent perioperatively or replaced with another type of plate. In four cases (4%) the lateral part of the plate was placed medially and vice versa. In 29 out of 55 (53%) complex fracture cases (OTA type 15-B2 or 15-B3) the plate had to be removed, measured in the period from 2010 till 2013 to accommodate a follow up of at least a year. In contrast, in only 9 out of 38 (24%) simple fracture cases (OTA type 15-B1) the material had to be removed within this period of time (significant difference, p: 0.005). This entails that the chance the material has to be removed due to irritation or worse is halved with simple fractures in contrast to complex fractures.

Furthermore, until 2010, standard reconstruction plates were implanted. Around 2011 they switched to precontoured clavicle locking plates. To assess the difference in outcome between these plates the outcomes were compared between 2010 and the period from 2011 to 2013. In 2010, 10 out of 19 (53%) plates had to be removed of the complex fracture cases, exactly the same ratio as in the following period, namely 20 out of 36 (53%). However, for simple fracture cases in 3 out of 7 (43%) the material had to

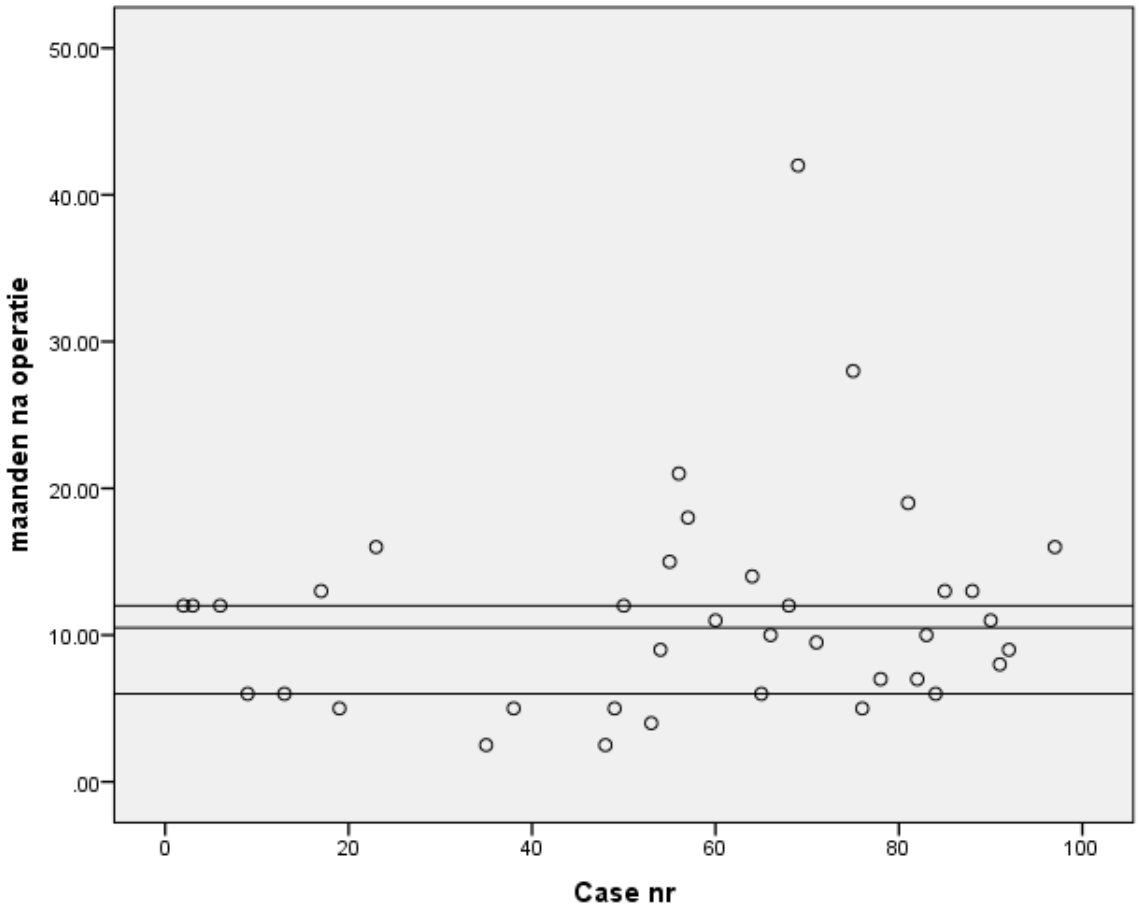

Figure 2.2: Scatter-plot of the number of months between surgery and plate removal. Reference lines situated on first, second and third quartile.

be removed in 2010, which is a factor higher than the 6 out of 30 (20%) from 2011 to 2013 (insignificant difference, p: 0.32). The difference was not significant due to the low sample size in 2010.

In this population, the biggest cause of a fractured clavicle with surgical treatment was cycling (45%).

Among the cases where the plate had to be removed the period between surgery and removal was evenly dispersed between 2.5 months and 16 with some outliers above. The median is around 11 months, the first quartile lies at 6 months and the third quartile at 13 months, figure 2.2.

2.3 Imaging

Rapid prototyping or 3D printing is a CAM method (computer aided manufacturing). Before one can manufacture something the computer has to be provided with a design. In healthcare this design, in most cases a computer aided design (CAD), can be obtained from medical imaging, which subsequently is segmented and modelled into a 3D object. In this section background of medical imaging acquisitionis described, which is the first step in this CAD process . The remaining steps will follow this section.

There are essentially two medical imaging modalities available for an effective visualization of bone in multiple planes, the three dimensions. These include Computed Tomography (CT) and Magnetic Resonance Imaging (MRI). In bone segmentation higher contrast and spatial resolution will result in more accurate results. Other techniques are available such as surface 3D scanning or 3D echo. However, in this case those techniques would not suffice, as they do not visualise the insideof the body in high resolution.

2.3.1 Computed tomography

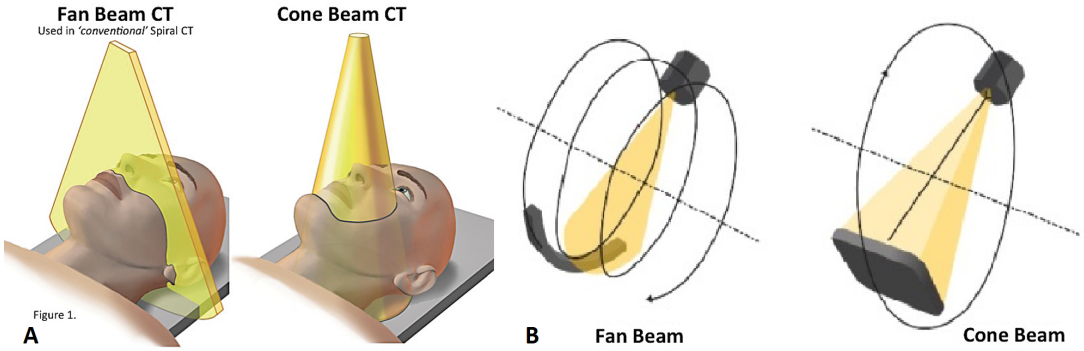

Figure 2.3: Graphical representation of the acquisition in computed tomography for fan and cone beam techniques. In A the difference in beam geometry is visible (www.oralhealthgroup.com). In B the difference in spiral rotation in standard fan beam CT modalities and the circular rotation in the cone beam modality (carestreamdentalblogdotcom1.wordpress.com).

In a similar way as with X-ray, CT uses radiation for visualisation. A homogenous beam is emitted through the object and detected on the other side. The structure with a higher radiation attenuation lets less radiation through, which defines the contrasts between different materials or tissues. However, CT uses multiple angles instead of a view from one angle to be able to reconstruct the object in 3D.

For CT there are two options; the conventional fan beam CT (CT) and the cone beam CT (cbCT). As the name suggests, the difference between the two lies in the shape of the beam, figure 2.3A. The conventional CT-scanner in Isala is the spiral fan beam CT. The modern versions have multiple rows of detectors, e.g. 64 to 256 rows, that smoothly rotate in a spiral around the subject, figure 2.3B. On each row a flat, two dimensional, fan beam of gamma radiation is transmitted from the source on the opposite site to an array, or line, of detectors. A half spin represents a slice in the resulting images. The cbCT uses a cone beam, which projects on a two by two matrix of detectors, a two dimensional plane. Comparable with a C-arm, it takes images from multiple directions and reconstructs transversal slices from these. CbCT is commonly seen in dental practices, but can also be seen in the hospital for acquisition of low dose anatomical data. For instance in Isala, a cbCT is integrated in the SPECT.

The cbCT produces a lower radiation dose compared to the conventional CT, but is more prone to artefacts and scattering which lowers the contrast. The signal to noise ratio (SNR) is lower in such a way that the rescaling to Hounsfield units (HU) cannot be applied. The contrast between bone and tissue is good, but a significant dose reduction can mainly be achieved in parts with little attenuation, like the head and extremities.

2.3.2 Magnetic resonance Imaging

In simple language, a MRI measures the (hydrogen) proton density, the number of hydrogen atoms per volume in tissue using magnetism and radiofrequencies. With different settings some molecules consisting hydrogen are highlighted more than others, based on their influence on the hydrogen atom. For instance, the size of the molecule of which the hydrogen atom is part of has an influence on how the atom is observed. This is how the contrast between water, a small molecule, and lipid, a large molecule, is achieved.

2.3.3 Conclusion

Bone does not contain any hydrogen in contrast to cartilage, which means that bone does not give any signal in a MRI and is depicted black. This in contrast to CT, which shows a high contrast between bone and surrounding tissue, figure 2.4. The scan time in MRI is longer than CT, but no radiation dose is produced. MRI is a valid option in cases where the cartilage needs to be taken into consideration in the segmentation. An example is the development of saw and drill guides for knee arthroplasty (e.g. VISIONAIRE ^{TM}). The standard MRI image resolution is half as good as a standard CT image. Better resolution can be achieved, however rapidly increases the acquisition time which increases the chance of movement artefacts.

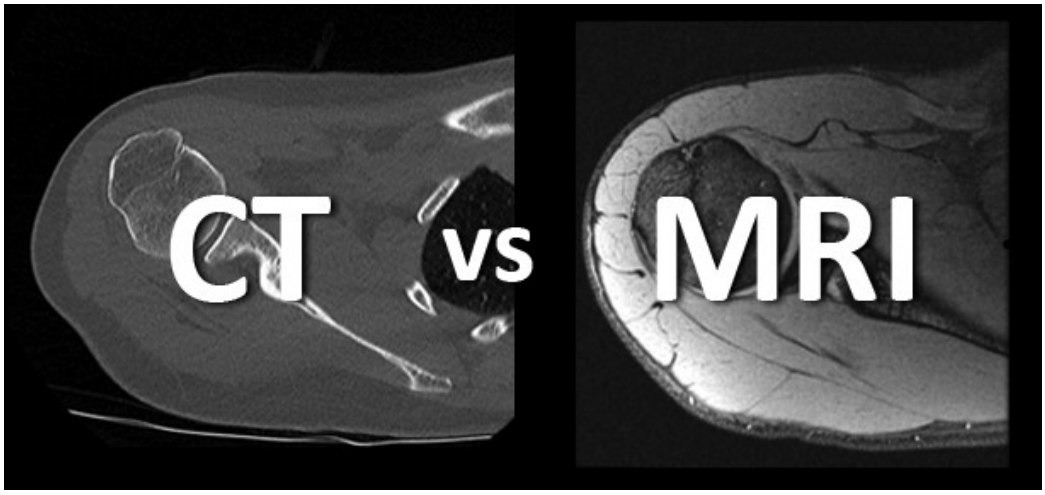

Figure 2.4: Graphical demonstration about the difference between CT and MRI bone visualisation. This is one of many visualisation sequences of the MRI.

To conclude, in most cases a CT is a valid modality to image bone structures. When the head or the extremities are targeted the cbCT will achieve the desired results; and for the remaining body the conventional CT is advised. MRI is a valid option when the cartilage is also important and when radiation has a more damaging effect (children).

2.4 Virtual processing

When the images are acquired the next CAD step is to process these images into an accurate representation of the targeted anatomical structure in 3D surface models. The processing can be roughly divided into the following steps. The first step is to segment the anatomical structure, here the bone, from the images, subsequently the segmentation is to be converted into a 3D surface mesh model, which can be cleaned and smoothed if necessary. The final step is to transform the model into readable code for the manufacturing machine, in this case a home-use 3D printer.

2.4.1 Segmentation

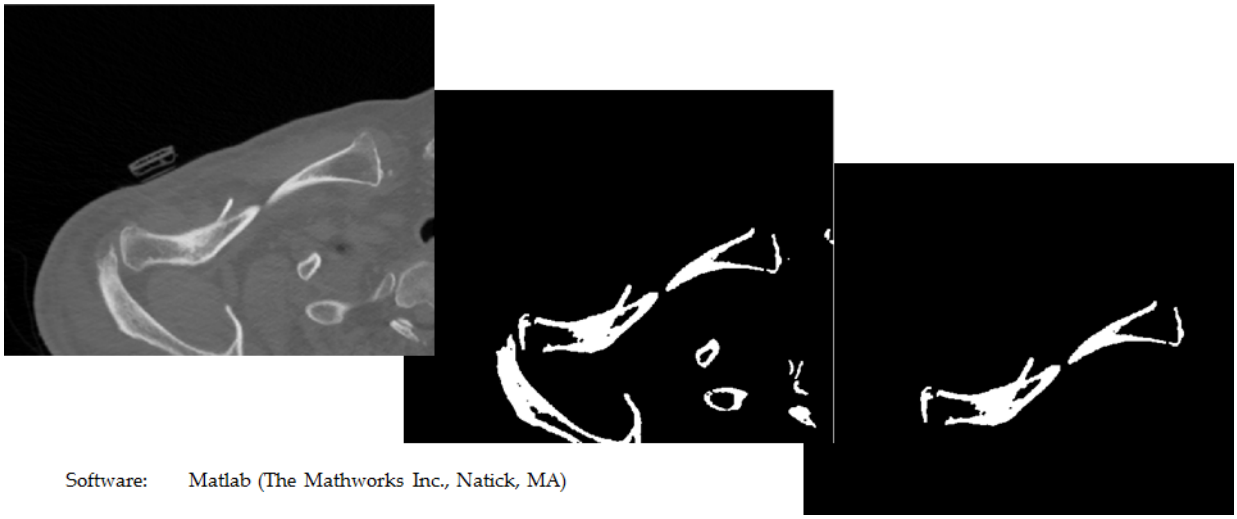

Figure 2.5: From left to right: A CT slice of a clavicle, the bone structures in the slice segmented with the thresholding technique, solely the clavicle selected with region growing technique.

Segmenting the bone from the images can be seen as cutting it out of every slice. Wikipedia defines it as followed:

> ”In computer vision, image segmentation is the process of partitioning a digital image into multiple segments (sets of pixels, also known as superpixels). The goal of segmentation is to simplify and/or change the representation of an image into something that is more meaningful and easier to analyse. Image segmentation is typically used to locate objects and boundaries (lines, curves, etc.) in images. More precisely, image segmentation is the process of assigning a label to every pixel in an image such that pixels with the same label share certain characteristics.”

There are multiple segmentation techniques and they can be categorized in manual, semiautomatic and automatic segmentation. In manual segmentation the user has to select the region of interest (ROI) by hand, by cutting the object out of the images, slice by slice. This is a very time consuming venture. Semiautomatic segmentation techniques make it a bit easier. Here, an algorithm supports the user in selecting the region of interest. This may imply that the user roughly selects the area and the algorithm searches for the edges. Or the algorithm supplies a rough estimation of the ROI based on the ROI in previous slices, which the user can then refine. One example is region growing where the user places a seed after which the algorithm searches for the connecting pixels in the object.

Automatic segmentation techniques work without specific intervention of the user, which makes it an objective method. Moreover, it is not labour intensive, thus saving the user time. The simplest example of automatic segmentation is thresholding 2.5. In thresholding voxels are divided by a certain threshold value and every voxel below or above this value is considered part of the ROI. It is fast and very convenient when the structure has a significantly higher pixel value than the surrounding structures, like bone or contrast agents in CT images. Some examples of more complex automatic segmentation algorithms are edge detection, like the water shedding technique, or principle component analysis (PCA). In PCA, like active shape modelling, the algorithm learned the shape of an anatomical structure with its possible deviations from a large database. It will search for the edges of the object within the known likelihood and limitations of the shape. The quality and ease of the segmentation is greatly dependable on the quality of the medical images. Most scanners have different validated algorithms and filters to reconstruct the raw data as accurately as possible. If the acquired data for segmentation, for example, contains a lot of noise a Gaussian filter can be used to reduce it.

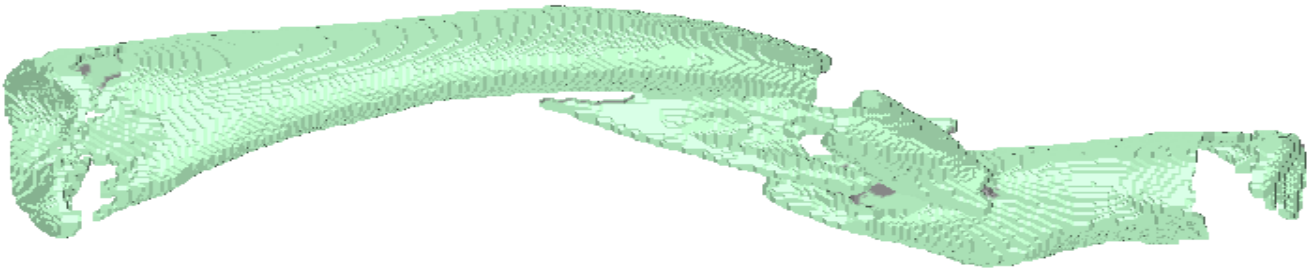

Figure 2.6: 3d image

Most of these techniques are part of the curriculum the track Medical Imaging and Intervention of the Technical Medicine course and are programmed using the mathematical software Matlab (The Mathworks Inc., Natick, MA). Besides programming, other options are available. Some radiology departments have software available for segmentation and 3D modelling; Isala is one of them. Further commercial software packages are available. One that is regularly mentioned in literature is Mimics from Materialize which is used in UMCG for mandibular reconstruction planning. Other options are Amira from FEI or EBS software from Ekliptik. In UMC Radboud the program Maxilim is used, commercial software which they further develop themselves. Alongside these commercial packages a lot of open source software can be found. The best known option is slicer.org, a project of MIT (Massachusetts Institute of Technology). Other smaller packages are also obtainable such as MITK or ITK-snap. The advantage of open source software is that it is free and can be used and further developed and adjusted as desired. The fact that it is not validated and there is no party standing by for backing you up or offering assistance in time of need, is a drawback.

2.4.2 3D modelling

The software packages mentioned above also have capability to be used for 3D modelling. After segmentation, the anatomical structure is stored as volumetric data. In this step, volumetric data is converted into a 3D model through volume rendering. One direct volume rendering technique is volume ray casting. Volume ray casting is the technique used by radiology to create the 3D images that can be viewed in the PACS client of the hospital. It uses the volumetric data to create a 3D image from the one view at a time using, as the name suggests, casting of virtual rays. The beauty is that different colour codes can be assigned this way for different densities, by using the internal data of the model instead of just the surface. Unfortunately, it is not possible to use the resulting file format for rapid prototyping. There are multiple options for rapid prototyping applications, but the common denominator is that they all compute the isosurface. An isosurface is a three dimensional isoline that represents the surface in the data of a constant isovalue. The marching cubes algorithm is the best known technique in this category. Matlab has a standard function called ”isosurface”, which computes the surfaces at a given isovalue. The result is a mesh consisting of coordinates, called ”vertices”, and triangles, called ”faces”. Three vertices define one face and the surface of al combined faces represent the surface of the targeted 3D model, figure 2.4.2 . The file format is .stl, short for stereolithography.

The next step is processing or editing the mesh, which can be seen as reversed engineering. A great range of CAD software is available for this application, e.g. Solid Works, autoCAD and Inventor. Unfortunately most CAD software is not built to work with large, detailed stl files. A better category of software suitable for editing .stl files is 3D graphic software, such as open source Blender , or paid Maya and 3dsMax. For this thesis the mesh processing software Meshlab is used for further editing.

When the 3D model is finished, the last step is to convert it to commands readable by the CAM

machine. This script is known as ”g-code”. Many professional machines have their own software. Many simpler machines utilize open source software, as Slic3r, Repetier and Cura. In this case we used Cura, provided by the 3D printer company Ultimaker. Prior to manufacturing, a couple of features have to be added to the model, depending on the manufacturing technique. In case of fused filament fabrication (see next section) a support structure is needed to avoid the model from moving or falling during fabrication. Furthermore, in order to increase the fabrication speed and reduce the amount of material the model does not need to be solid. In this step the shell thickness and filling density can be determined. When the model is ready to be fabricated, the model is again sliced up in layers representing cross-sections of the model. Every move and action of the machine to construct the object again, is translated in g-code commands.

2.5 Rapid prototyping

Rapid prototyping is a group of techniques that has the collective property of adding material in contrast to subtractive production processes, like milling, turning or drilling. For engineers, this makes it just one of the production machines in the workplace. Similar terminologies for rapid prototyping are additive manufacturing, additive fabrication and 3D printing. The term rapid prototyping implies that the technique is suitable to produce a prototype or design in a timely manner. To create a physical version of digital designs, rapid prototyping machines are controlled by computers, which makes rapid prototyping belong to the category of CAM, making the CAD/CAM concept complete in combination with the previous sections. Many different techniques are available, each with its own advantages and disadvantages. Each technique varies in multiple parameters, such as cost of machine and material, building resolution, size and time, and material type and properties. There is a big difference in quality and costs between commercial available machines for home-use and industry. In this section an overview of techniques useful for this field will be given, divided into three categories: solid-, liquid- and powder-based.

2.5.1 Solid-based

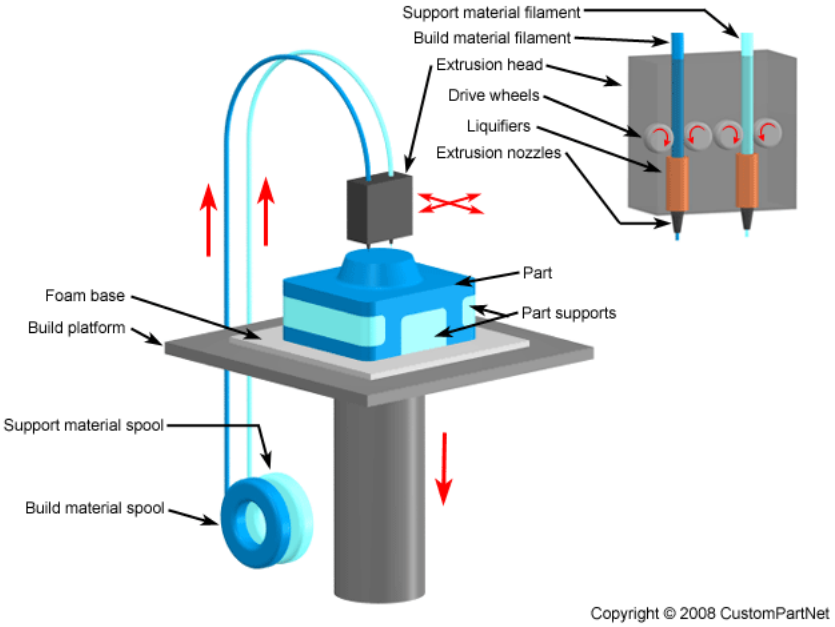

Figure 2.7: Graphic representation of the Fused Deposition Modelling (FDM) technique. Source: www.custompartnet.com

Fused deposition modelling (FDM) is the most commonly used technique in current home-use machines. It is also known as fused filament fabrication. This term was created due to copyright issues of FDM in the 3D printing community. Like all techniques in this section, FDM creates a 3D model by building it layer by layer. Each layer is composed by depositing molten plastic from an extruder (print head) and cooling it instantly. A videographic representation of this process is presented in chapter 3, figure 3.2. Most machines move the extruder in the xy-plane and lower the printing bed after each layer in the z-direction. The manner to build up the model in 3D may vary between machines. The fabrication materials are different kinds of plastic. The most commonly used plastics are acrylonitrile butadiene styrene (ABS) and polylactic acid (PLA). In many machines the plastic is fed through the extruder as a wire from a spool; another option is in the form of granules from a container. This wire is pushed through a heated element just above melting point and after extrusion cooled quickly with fans to attain its proposed shape. Figure 2 depicts a graphic representation of FDM.

Layers need support when there is overhang in the model. A slope with an overhang exceeding 60% can cause faults in the product, which could be prevented by an added support structure. This structure can be made from the same material as the rest of the model and removed afterwards by hand or this structure can be dissolved in water by using a second, water-soluble polymer, like poly(vinyl alcohol) (PVA). Unfortunately, not all machines are capable of using two materials in one print. Figure 2 is a graphic depiction of FDM with one technique of using 2 materials.

Costs for a home-use printer ranges from 500 to 3000 euros and the standard materials are available from 20 to 40 euros per kilogram. Prices for professional industrial printers start around 20.000 euros and the material costs are also significantly higher. The highest resolutions are around 0.1 mm in the z-direction and 0.4 mm in the xy-plane. Printing speed is around 60 mm per second, which is relatively

slow with around one hour for a simple object. Another less commonly used technique in this category is laminated object manufacturing (LOM). In this technique, each layer is cut out a sheet of a certain material and stacked in order to create the three dimensional product.

2.5.2 Liquid-based

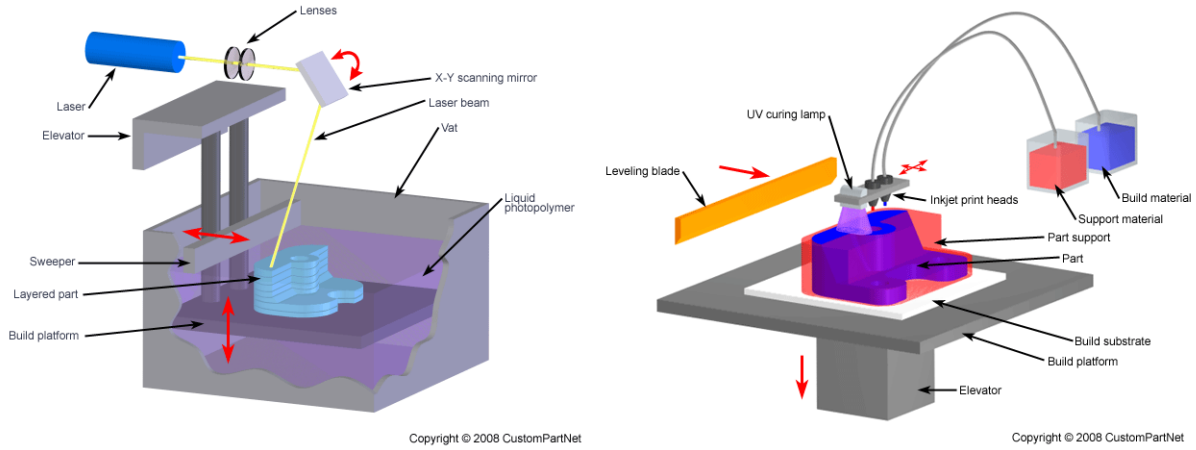

Figure 2.8: Graphic representation of stereolithography (SLA), with top up method to the left and photosensitive inkjet printing, with two materials to the right. Source: www. custompartnet.com

In this category the techniques can be roughly divided into stereolithography based techniques and inkjet printing based techniques. In the late 80s, stereolithography (SLA) was the first technology to be introduced for rapid prototyping and has been much developed since then. In SLA, a liquid photosensitive resin is hardened, or cured, layer by layer by means of a low-power, highly focused UV laser. In each layer the laser can solidify the cross-sections of the 3D model very accurately. From here an SLA machine may vary in design. For example the machine may use the top-down or top-up method, in which the model is printed upside down and pulled up out of the resin vat, or the model is printed on top of the printing bed and is lowered and immersed in the resin vat. The latter technique is depicted in figure 3.

Recently, SLA home-use versions have become commercially available for around 3000 euros, with material costs still decreasing and currently around 70 to 400 euros per kilogram. With a resolution of 0.05 to 0.15 mm, SLA offers a slightly higher resolution and is slightly faster than FDM. A new development is a variation on SLA and is called direct light processing (DLP). Instead of one UV laser beam a two dimensional image is instantly cured (hardened) with a UV projection. In this method, the resin can be cured per layer or continuously, resulting in a smooth transition between layers. As the resin is not cured pixel for pixel but as a whole at once, this drastically improves printing speed while retaining the original quality of SLA.

The inkjet printing technique is related to the 2D paper printing technique, where drops of ink are deposited. For three dimensional structures, droplets are deposited layer by layer, representing the cross-sections of the 3D model layer by layer. The trick is to solidify these droplets and for this, multiple methods are developed. A relatively simple option is using molten polymers which are instantly cooled after deposition. Another option is to add an agent after deposition that reacts with the droplets or after exposure to heat or light. The most commonly used method is using liquid photosensitive material, similar to SLA, and harden each deposited droplet or layer by exposing it to UV light, figure 4. Deposition of droplets is a slow process compared to the other techniques, unless an array of nozzles, or print heads, is implemented of the entire width of the print bed . This way the nozzles move only in one direction and deposit an entire layer in one go. This technique is called polyjet of multijet printing depending on the providing manufacturer.

The advantage of inkjet printing is its possibility to deposit an extra material by implementing two nozzles. A second material is often used for support. Wax is an example of a support material.

2.5.3 Powder-based

This method binds powder together, again layer by layer, each representing a cross-section of the 3D model. After one layer is completed a new layer of powder is dispersed equally on top of it. This can be done with, for instance, with a roller. The roller pushes or rolls out powder from the supply chamber which bottom raises the powder when the building platform is lowered in a similar fashion as previous techniques, see figure 2.9. The benefit of this technique is that the remaining powder acts as support and no additional support structure or material is necessary. There are two methods of binding the

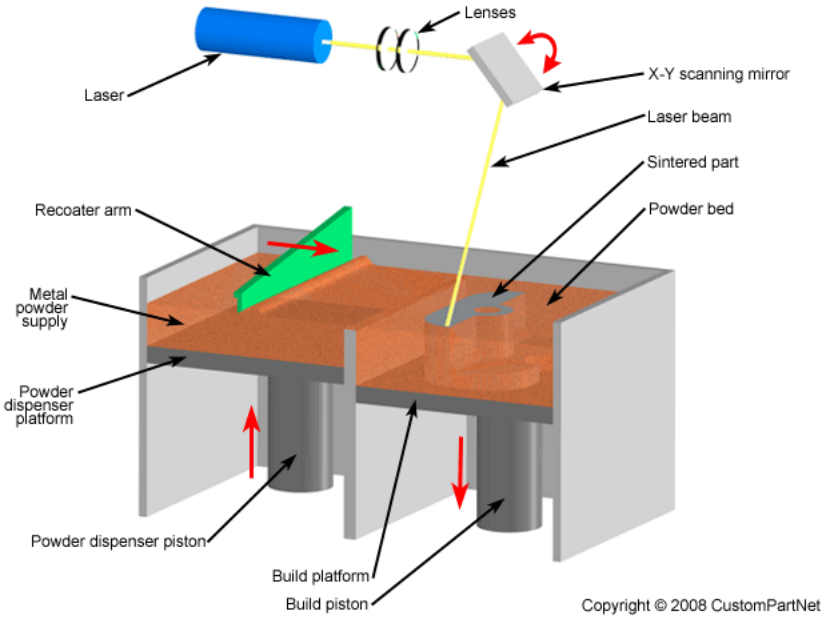

Figure 2.9: Graphic representation of direct metal laser sintering (DMLS) and its powder distribution. Source: www. custompartnet.com

powder. The technique's selective laser sintering (SLS) and direction metal laser sintering (DMLS) melt the powder together, whereas in three dimensional printing or colorjet printing a liquid adhesive is used to bind the powder.

SLS and DMLS use a high power laser in the same manner as SLA, to melt the powder selectively on the predetermined locations. In SLS available materials are polymer and metal composite powder. In case of the metal composite, the polymer binder powder mixed in the metal power will be solidified. In post-processing the product is heated in an oven in which the polymer will be burned off and the resulting space is infiltrated with bronze to increase density. But even with infiltration only a density of roughly 70% is achieved. DMLS uses finer pure metal powder and a high powered laser to solidify the metal powder directly, so no post-processing is needed. With DMLS a density around 95% can be achieved. SLS is a fast technique resulting in material with excellent mechanical properties; however, for metal printing DMLS exceeds SLS in mechanical properties. Only industrial machines are commercially available and the machines and materials are very expensive. A DMLS machine ranges from 200.000 to 1 million euros.

Of all techniques, three dimensional printing (3DP) or colorjet printing is the most comparable to conventional paper 2D printing. However, instead of a sheet of paper, a thin layer of powder is used as base. The types of material are somewhat limited, but like the ink in a standard printer the adhesive, or binding liquid, comes in many colours. This results in a full colour printing capability. The result does not have the finest surfacing and low mechanical properties, but it is a very fast technique, as it is again possible to implement an array of nozzles.

Chapter 3

ClaRP: Method

In this chapter the technical protocol is described and the choices in material and techniques are explained. An overview of materials and techniques is given in previous sections, and the implementation will be given in section Design.

3.1 Technical protocol

3.1.1 Image aquisition

The details of the CT protocol are stated in Appendix D. The protocol is based on an existing CT protocol for 3D visualisation of the shoulder, used to evaluate the bone structures of the clavicle, scapula and humerus. The used settings and filters were specifically developed by the manufacturer, Philips, for volume rendering. The targeted rendering technique for this protocol was volume ray casting. Volume ray casting is a different rendering technique than used in the virtual processing in for the ClaRP trial, but the requirements are similar. The most important requirements are, as expected, no artefacts, high resolution and strong contrast between bone and surrounding tissue. In the end, a customization of the 3D shoulder protocol is made for the ClaRP trial. To lower the dose the mean X-Ray tube current is halved and the scan length is shortened to the bounds of the clavicle, around 10 to 15 cm. The original protocol was to reconstruct both clavicles separately from the raw data. This process was deemed to be too labour intensive and time consuming for the radiology operator. Instead, both clavicles were reconstructed at once from the raw data with a large field of view (FOV). From this reconstruction both clavicles were cropped. The pixel dimension of the images is directly proportional to the matrix size, originally 512 by 512, and the FOV, or rather the reconstruction diameter. Thus with the FOV twice as large, so are the pixel dimensions. In consultation with the protocol writer some adjustments were made to the protocol at time of the fourth subject. The radiology operators did not need to crop the images, as this step was also included in the virtual processing. And the matrix size settings were increased to the maximum of 1024 by 1024. Because each patient differs in diameter and the operators had to determine the FOV manually, there is some variation in FOV and thus pixel dimensions between subjects. The data collection diameter in this specific CT-scanner is 500 mm, which means the dimensions would never be lower than 0.49 mm (500 mm/1240) in xy-plane. The resulting dimension averaged at 0.45 mm, which is accepted for this study.

3.1.2 Virtual processing

After the CT images were acquired in the form of DICOM-files (Digital Imaging and Communication in Medicine), they were virtually processed, which means segmentation, volume rendering and conversion to 3D printable objects. Segmentation, visualisation and modelling is part the curriculum of Technical Medicine in the track Medical Imaging and Intervention. Within the curriculum, the students obtained a toolkit of techniques and learned to implement them in mathematical software Matlab. For this reason, MatlabR2014b (The Mathworks Inc. Natick, MA) is used for the first part in processing. Plus, by doing so, the researcher is aware of every processing step made, because he is in control of the programming. This way, the issue is traceable if something unforeseen happens. Within Matlab a program with a graphic user interface (GUI) is written. A screen recording of this program is shown and the following processing steps is in figure 3.1.2. The pseudocode of this program can be found in Appendix C. In the reconstruction software of the CT scanner different validated filters are integrated. For this reason, preferably no filter is used on the CT images prior to segmentation to ensure validated data, although there is a Gaussian filter integrated in the program in case of obstructing noise. The automatic segmentation method thresholding was sufficient. Automatic segmentation is preferred as it is less time consuming and thers is no inter-operator variability.

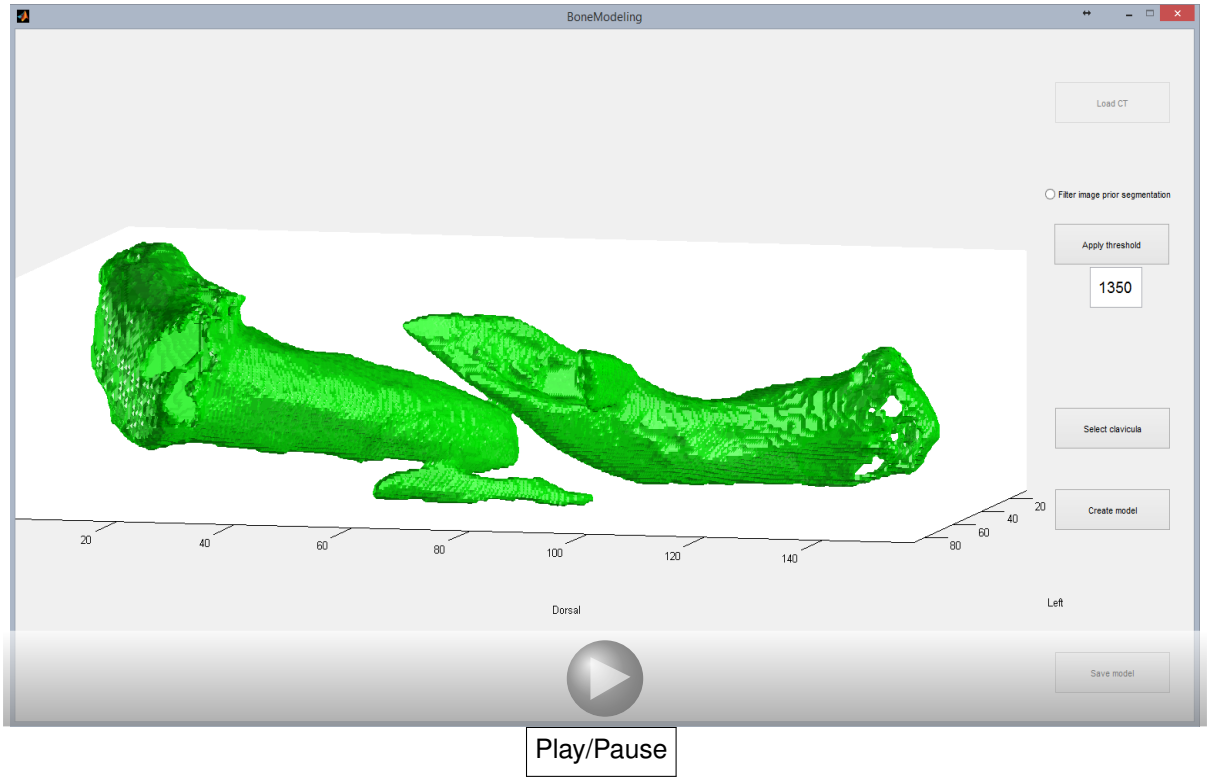

Figure 3.1: Video graphic impression of the virtual image processing.

For thresholding, only the variable threshold value is needed. In a validation study with a lamb's shank, next section Bone validation, the threshold value is selected as close as possible to the reality, resulting in an intensity value of 1300, which relates to 300 Hounsfield units. The threshold was determined on the targeted surface, the midshaft, as this was prerequisite for fitting the plate. The distal and proximal ends of the clavicle, unfortunately had a lower density, which resulted in parts that were not included in the segmentation. This created holes in the 3D model, also visible in figure 2.4.2

The standard function isosurface in Matlab is used to compute the 3D mesh model, as explained in section 2.4.2.The faces separate the segmented bone from the surrounding structures. Matlab is not built for further processing these meshes. So instead, the advanced 3D mesh processing open source software Meshlab (Visual Computing Lab, Pisa, Italy) is used for the following steps where holes are filled, fragments are separated and the normals of the faces are uniformly oriented outwards. At this point the layers of the CT scan are still visible in the mesh and it could contain corruptions, such as holes, manifolds and double vertices. Using the points and normals, a new smoothed surfaces is reconstructed using the Poisson reconstruction approach.

3.1.3 Rapid prototyping

The rapid prototyping device used in the ClaRP trial is the low-budget Witbox Bq 3D printer (Appendix E), an FDM machine with a relatively large print bed, suited mainly for polylactic acid (PLA) as print material and able to use only one material at the time. Before the 3D mesh model is suitable for fabrication a support structure has to be added. Subsequently, the inside has to be defined and converted into layers. Witbox is compatible with multiple open source softwares. For sake of convenience Cura 15.02.1 (Ultimaking Ltd., Geldermalsen, Netherlands) was used, because different researchers in other centres, such as the University of Twente, work with the FDM machine Ultimaker, which also uses Cura. In Cura the model of the bone and fragments are loaded and positioned in such a way that they lay as flat as possible, to win time, with the cranial side up and the contralateral healthy clavicle is mirrored. Subsequently, the positioned models are provided with support structure and filling. In the end of video 3.1.2 and 3.2 can be seen how the inside of the model is filled. The specific settings are given in appendix F. The settings are set to the lowest quality, because a higher quality is not necessary for this application and thereby speeds up the fabrication significantly. The final step is to convert the whole structure into layers, script it to a g-code and load it on a SD card.

The SD card can be plugged in the Witbox. The print bed has to be levelled, the (white) filament loaded, after which the print can be started. In figure 3.2an end result of clavicle fragment is shown shortly after the 3D printer was finished and a videographic example is presented of a model being printed half way through. To encourage stable adhesion to the print bed a layer of kapton tape is fixed upon it. Depending on the size, especially the height, number of fragments and the setting in Cura,

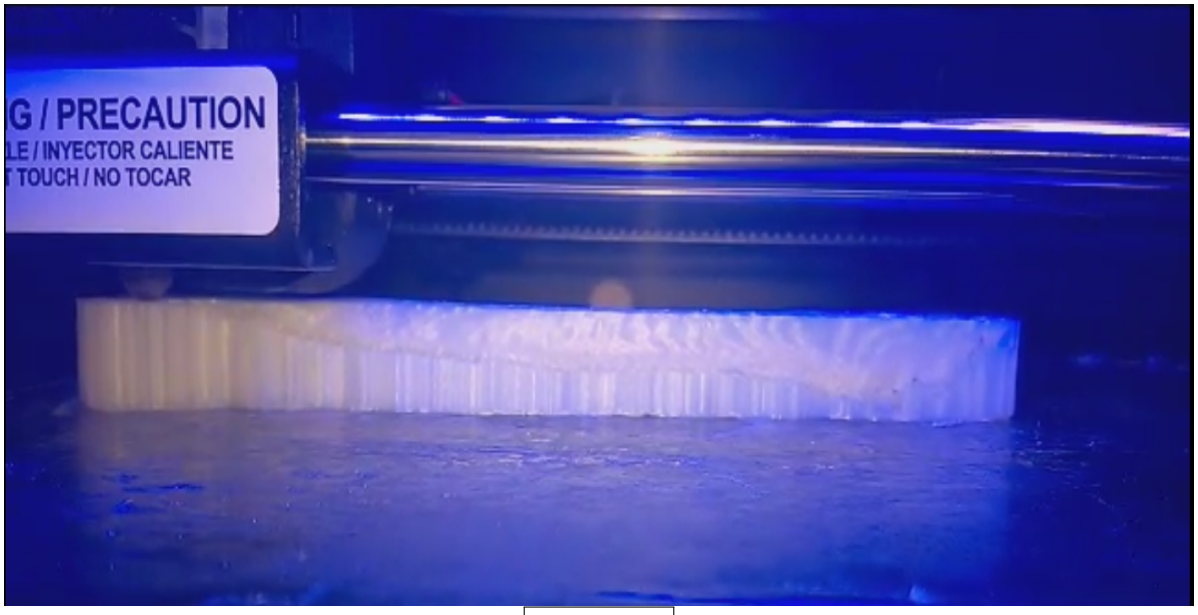

Play/Pause

Figure 3.2: Poster image:A clavicle fragment shortly after the 3D printer finished. Video: Short video of how the Witbox 3D printer builds a model.

the fabrication time is between 60 and 100 minutes, if nothing fails. A common failure is the model loosening from the printing bed during the process. The highest chance of this failure occuring is in the first couple of layers. Another failure is when, due to unknown reasons, the x- and y-coordinates shift and the following layer shifts in position. It is advised to be alert during the fabrication process in case of failure. When the print is ready, the support structure can be removed by breaking it off. The remaining model will be rough on the bottom due to overhand in the support structure. This roughness can be polished smooth.

3.1.4 Plate manipulation

Figure 3.3: On the left: is the set depicted with the forceps and a bent plate ready for sterilization. On the right: are two bending irons used for the rotational adjustments.

The plastic models are now ready to be used for bending the plate according to their shape. An easy tool for the reduction of the fractured model is clay, figure 3.1.4. The mirrored model is pressed in the clay so that the created shape in the clay could be used as a mould for the reduction. The fracture lines were drawn on the mirrored model and positioned behind the fracture model to create an ideal set-up for fitting the plate.

The choice of plate was based on a set of fitting plates. The original set-up was that a new sterile version could be obtained perioperatively when no bending was needed, in case the fitting plate already had the right curvature, this would the additional sterilisation. Unfortunately, the set with fitting plates that was borrowed from the manufacturer Synthes DePuy, consisted of superior clavicle plates instead of the superior-anterior clavicle plates, that are used in the operating room (OR), due to a misunderstanding. This meant that accurate testing with these fitting plates was not possible. However, an indication on the type of plate, left or right and length could be based on these fitting plates. A sterile version of the established plate type had to be acquired, together with the irons and pliers for bending, left figure 3.1.4

Figure 3.4: On the left: is the setup in clay depicted with fracture drawn on mirrored model, outlines of the plate and the fitted plate. On the right: are two models visible. Both are the same fractured model, except left is before and right is after bending. It can be seen that the plate on the left model does not fit the curvature of the model to fixate the fracture properly.

To place the plate on a tactical position a few considerations needed to be taken into account. For solid fixation, three screws on both ends are preferable. If this seems impossible at least two screws are necessary to prevent pivoting. Through the surgical approach only the anterior and superior surface of the clavicle can be reached. The placement of the plate needs to be limited to these surfaces combined with the fact that proximally the head can be a hindrance for drilling the screw hole. Prior to placement of the plate, perioperative reduction of the fracture would take place. During the reduction different materials were used, namely forceps, screws and k-wires. A good understanding of the reduction can help to predict the placement of these materials. The placement of these instruments was taken into account during the preoperative bending, see figure 3.1.4, to avoid that these instruments would perioperatively obstruct correct placement of the plate. Pointy forceps are available perioperatively for fixating the reduction; these forceps leave enough space for a plate.

On the plate an indication is present that states which side is supposed to point laterally. When the fracture is situated relatively laterally the curve in the centre of the plate will not relate to the bone any more. In this case this indication should be inversed to medial. It is possible to manipulate the plate in multiple directions, to bend it sideways and up or down or to twist/rotate the plate.

Most of these pointers were learned in the process during the ClaRP trial. In appendix G is stated what was learned during which case.

3.1.5 Finish

When plate manipulation is completed the plate was outlined and the holes were marked on both models, figure 3.1.4. With the fitted plate and a calliper the length of the locking screws were measured, by measuring the thickness of the plate and model combined perpendicular on the tapped screw hole. When determining the screw lengths for perioperatively placement, they should rather be 2 to 4 mm too long than too short. For that reason the lengths were rounded up to an even number of millimetres with an additional 2 mm.

Pictures were taken of the models with outlines and the placement of the plate, figure 3.1.4, and documented together with the proposed reduction and screw lengths for the performing surgeon.

The plate was manipulated on the OR complex, because here sterile versions of the plate and instruments were present and to finish the plate had to be placed here in a net, figure 3.1.4, for sterilization. A specific protocol for sterilization was set up for this trial. The protocol extends outside the prescribed accountability of the material, so a physician, in this case the primary surgeon, has taken responsibility. The signed protocol is attached in appendix H. The central sterilization administration (CSA) needed 11 to 24 hours to have it back on the OR again.

Figure 3.5: On the left: is the principal investigator depicted while bending a plate and on the right the caliper while measuring a screw length on a fractured model.

3.2 Bone study

The technical protocol was tested in a pilot case, which gave the confidence to continue to a clinical study. In the pilot case the plate fitted, but this did not prove that the printed bone was a correct, direct replica of the bone. Questions arose about the validity and precision of similarities between the bone and the replica. Errors and deviations could occur during imaging, segmentation, volume rendering, post processing and fabrication. CT-imaging is a well validated and researched modality, however, different quality settings are possible and usually not the highest settings are used as ALARA is aspired. ALARA is an abbreviation for as low as reasonably possible and applies to the dose. Furthermore, as described in section imaging, there are multiple techniques for segmentation and volume rendering. Each process is an interpretation of the structure and in each step the errors of the previous steps are included. By programming the virtual processing in Matlab, most errors and deviations are known and taken into account. However, the exact severity of the combined errors is not charted.

3.2.1 Objectives

The institutional review board had the same question about the dose and validity of the method. For that reason, a bone validation study was conducted with the objectives to assess the loss in detail and information in the four transitions: imaging to segmentation to volume rendering and post processing to fabrication. All with different dosages with different modalities to evaluate the lowest dose possible (ALARA) while still remaining the guarantee for a valid replica of the anatomy.

3.2.2 Materials and method

To validate the technical protocol a validation study is performed with a lamb's shank, to simulate a human clavicle, with a cow's hoof for attenuation, figure 3.6. The goal was to test the errors and deviations in the conversion from cadaver to CT-images, from these images to a 3D model and from this model to a physical replica.

The spiral fan beam CT protocol was tested on different tube voltages, 100 or 120 kV, and varying tube currents (mAs). The standard settings of the 3D shoulder CT protocol were 120 kV and 200 mAs. The more detailed settings were copied from this protocol, because it was designed for volume rendering the bone structure in the shoulder. The protocol used a function to change the tube current proportional to the size of the subject at that specific cross section to accommodate for a similar image quality over the entire length. The set tube current, originally 200 mAs, can be set to a calibrated value, which is computed from a phantom with a diameter of 32 cm. If the cross section deviates from the phantom the tube current is adjusted accordingly. In the standard 3D shoulder protocol the calibrated current was set to 200 mAs and for the validation study the protocol was tested at 125 mAs and lowered

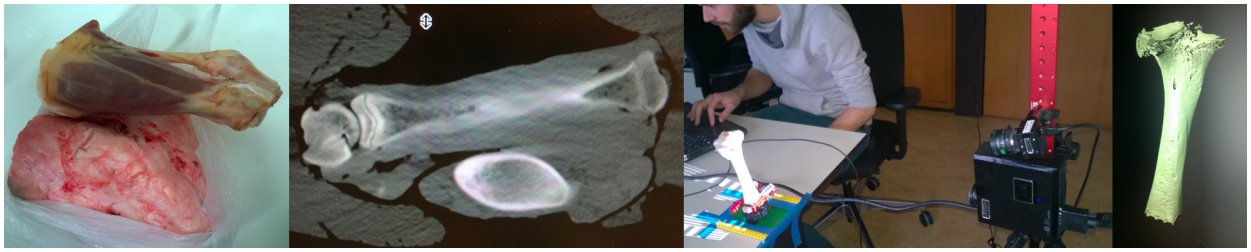

Figure 3.6: From left to right: the lamb's shank and cow's hoof with soft tissue, slice from CT scan, 3D scanning the shank using light projection, 3D foto from one side.

or heightened according to the image quality. In the end the bone was measured with currents of 200, 125, 100 and 50 mAs before running out of time.

With the aim to reduce the dose in the CT protocol, a cbCT was included in the validation study. The cbCT software and settings are not as advanced as on the standard CT. The general disadvantage of cbCT is the fact that the scale cannot be standardized to Hounsfield Units. Furthermore, it has only a couple of tube current settings, namely 5, 10, 20 mAs and then right up to 80 mAs and a voltage of 120 kV. Because the beam is a cone the scan length must be a multiple of 15 cm, which is actually perfect. The scan time is significantly higher, around 10 times, therefore, a current of 80 mAs will increase the dose in contrast to the standard CT and so 20 mAs is the maximum setting for the current to be beneficial. To compensate for the lack of attenuation around the cadaver, two plastic bags filled with water were placed on both sides of the cadaver. The same set-up with the exact same bags and content were used in the standard CT protocol. Unfortunately, after the CT scan, it became clear that the attenuation was overestimated by using the bags with a factor three. However, due to a tight schedule, there was no time left to redo the scanning. The bone had to be dissected from the surrounding tissue in order to be able to make a 3D surface scan of the shank.

To create a gold standard 3D model, the shank bone was cooked and separated from the surrounding tissue to be able to 3D surface scan it. At the University of Twente two 3D scanners were available on short term. The Konica Minolta Vivid 910 in the virtual reality lab, a professional laser-projection based scanner, and a DAVID SLS-2 used by a biomedical engineering (BME) graduate, a less professional light-projection based scanner, figrure 3.6. Together with the BME graduate, Johannes van Wijngaarden, the bone was 3D scanned with both scanners. Due to the expertise of the BME graduate with the light-based scanner, this model was highly detailed in contrast to the laser-based scanner. Thus the 3D model created with the light-projection based 3D scanner was included in the validation study as gold standard.

All data was processed in Matlab with different threshold pixel values, 1250, 1300 and 1350, respectively 250, 300 and 350 HU . The different resulting 3D models were aligned with the gold standard in Meshlab, with aid the of the alignment tool, first by using the Point Based Glueing and subsequently the Process options. After aligning two models the distance deviations were mapped. The distance was calculated in Meshlab based on the mathematical Hausdorff distance method. This method compares the point clouds, vertices, of the two models. Basically the closest vertex of the gold standard model is searched for each vertex in the targeted model and this distance is added as variable to that specific vertex of the test model. From the entire point cloud, every vertex of the targeted model, the minimal, maximal, mean and root mean square (mean+ standard deviation) distances were calculated. Furthermore, based on the added distance variable in the vertices, the targeted model was RGB colour -coded with red to green to blue respectively 0 to 9 millimetres. An example is shown in figure 3.7.

To define the best threshold value scans with the highest dose from the CT and cbCT were segmented with different threshold values: 1250, 1300 and 1350. The resulting models were compared with the 3D scanned model as gold standard. Subsequently, the models from the lower dose CT protocols, segmented with the resulting threshold value, were compared to the gold standard. The ends of the shank were taken out of account in the calculation, because they contained a large amount of cartilage, which is included in the model with 3D scanning, but excluded with segmentation. Furthermore, the ends were jointed, which means they were close to a different bone structure, which creates a misrepresentation. These two reasons combined with the fact that in the ClaRP trail only the shaft of the clavicle will be utilized, resulted in the decision to only analyse the shaft of the shank. Besides that, there were holes in the shaft caused by a partially relatively low density. From experience we know that this does not occur in the shaft of clavicles and if this did occur they would be filled, or reconstructed, so these holes were also cut out of the mesh. The results were shaft surfaces as can be seen in figure 3.7.

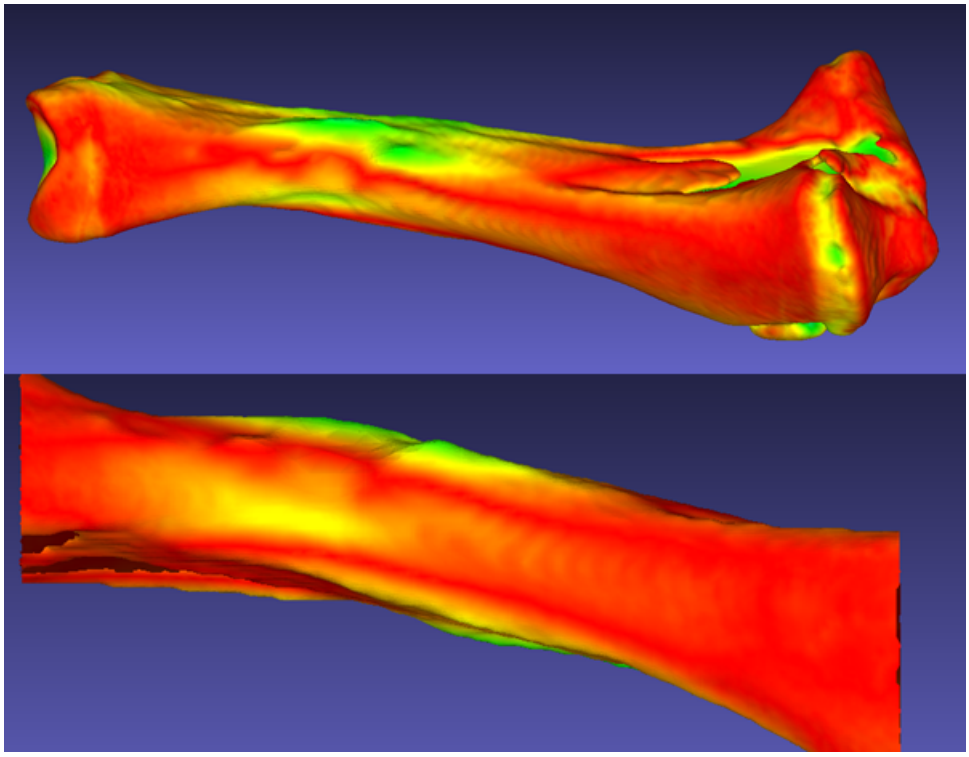

Figure 3.7: Colourmap after the Hausdorff distance computation at 100 mAs. Above of the whole shank and below of the just the shaft after hole removal.

3.2.3 Results

Although the scans from the cbCT without attenuation correction look really promising, the scans with attenuation correction showed such severe scattering that no reasonable 3D model could be generated. Because of this and later discussed reasons these were not further analysed . The standard CT 3D shoulder protocol deviated maximal 6.56 mm and on average 1.57 (SD 0.44 mm). Lower dose protocol results were: 50 mAs protocol maximum of 6.55 mm and on average 1.34 (SD 0.41 mm), 100 mAs maximum of 5.07 mm and on average 1.04 (SD 0.34 mm) and 125 mAs maximum of 5.86 mm and on average 1.07 (SD 0.40 mm).

Table 3.1: Results of the Hausdorff distance deviations.

Whole shank [mAs (threshold value)]	Max [mm]	Mean [mm]	rsm [mm]
200 (1300)	10.37	1.2	1.89
125 (1350)	10.32	1.33	2.04
100 (1350)	10.29	1.34	2.01
50 (1300)	10.35	1.35	2.11
Shaft shank [mAs (threshold value)]	**Max [mm]**	**Mean [mm]**	**rsm [mm]**
200 (1300)	6.56	1.57	2.11
125 (1350)	5.86	1.07	1.47
100 (1350)	5.07	1.04	1.4
50 (1300)	6.55	1.34	1.85

3.2.4 Conclusion

Based on this short validation study the technical protocol was adjusted, as imposed by the institutional review board, to the 3D shoulder protocol on the spiral fan beam CT with halved exposure and a threshold pixel value of 1300.

3.2.5 Discussion

Due to time pressure from the institutional review board (effective two and a half weeks), this study was performed suboptimally. In an ideal case the cadaver would be a human clavicle, but that is expensive and hard to come by on a short term. Unfortunately, most mammals are not in possession of a clavicle. That is why, in consultation with the local butcher, a lamb's shank is chosen with a free of charge cow's

hoof for attenuation. In the scan protocol the main objective was to test different modalities with different exposures. At first the hoof would be sufficient to compensate for the attenuation, however, in discussion with a clinical physicist from nuclear medicine, the bags of water were added to increase attenuation. These caused too much noise and artefacts, which were attributed to the fact that the trunk of the body in general would cause to much attenuation. The day after, the shank was scanned with a standard spiral CT with the very same bags of water, in retrospective the shank also should have been scanned without these bags for a proper evaluation of the data.

Further, the analysing method with distance mapping was not yet fully crystallized and in the limited time left, not all models could be generated. This, plus the fact that the noise and artefacts in the data from the cbCT were really obvious, and that the spiral CT is logistically convenient, led to the fact that the cbCT data was not analysed. After reporting it to the committee, the unattenuated cbCT data was investigated and showed superior results with a maximum of 2.03 mm and a mean of 0.33 mm (RMS: 0.40 mm) for the lowest dose of 10 mAs. Unfortunately, the results were interpreted incorrectly at the time. The standard and 50 mAs protocol was segmented at 1300 pixel intensity and the 100 and 125 mAs protocol were segmented at 1350 pixel intensity. This explains the difference in results. After evaluating this misunderstanding it also appeared a better option to set the standard threshold value to 1350 instead of 1300. In agreement with the primary surgeon, based on the available information, the distance deviations in the 100 mAs CT protocol were deemed acceptable. So this adjustment in the protocol was reported to the medical ethical committee.

In the end not the entire goal was achieved. The errors and deviations in the conversion from cadaver to CT-images, plus the conversion from these images to a 3D model were tested approximately. However, essentially these combined steps were tested and the conversion from this model to a physical replica was not tested at all.

3.3 Phantom study

The bone validation study in its entirety was pushed through in a rather short time span of less than 3 weeks, with the objective to facilitate the institutional review board with an answer. As stated in the discussion, not all the goals (section 3.2.1) were achieved in the bone validation study. To objectively investigate these conversions a phantom is designed in four parts to investigate four distinctly possible errors, seen in figure 3.3.

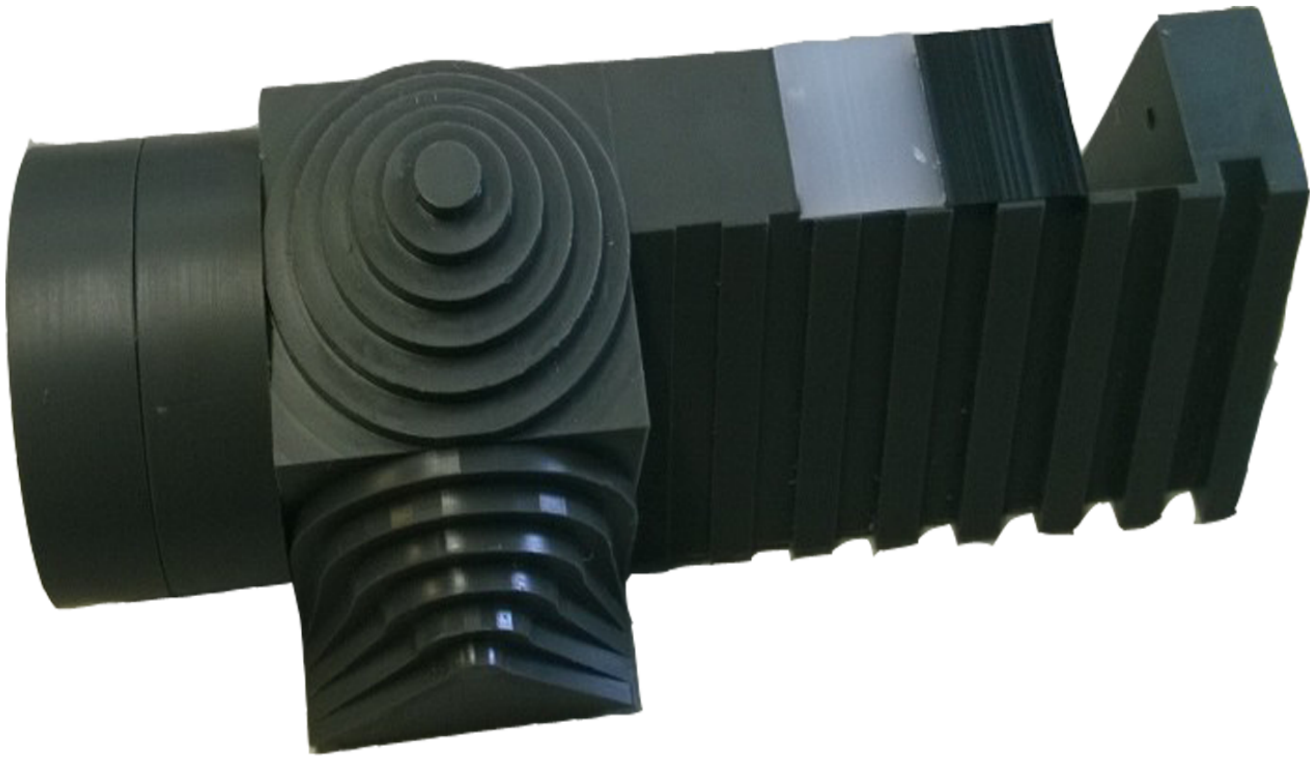

Figure 3.8: 3D image of the phantom fully assembled. Click to activate 3D view.

3.3.1 Materials and method

The first part is the pyramid of circles, figure 3.3.1 view ”Pyramid” . These are to test if the fabricated object will print in the same scale in each of the three directions. If not, an ellipsoid will form, which is easily measurable with a calliper. Plus, the gradually smaller circles will test how the virtual processing handles the conversion of voxels, which are basically cubes, to round circles and at what diameter this begins to show. This transition in voxels is again tested at different angles towards the bottom varying from 90 to 45 degrees in five steps.

The second part are the steps, formed like stairs, each with an added 0.2 mm difference to the one before, figure 3.3.1 view ”Stairs”. It was expected that the pixel dimensions of roughly 0.5x0.5x0.5 mm would not register the first steps. With this part the height at which the step is fully registered and correctly modelled can be objectively determined. The steps are built in at 60 degrees angle to avoid accidental overlap with the voxels, when placed horizontally, vertically or in at 45 degrees angle.

The third part is on the other side of the triangle, for the same reason as before at a 60 degrees angle. These blocks are shown disassembled in figure 3.3.1 view ”Triangle blocks”. Two of these triangle blocks are fitted against the slope, each made of a material with between the 200 and 300 Hounsfield units lower. In this manner the transition between different radiation densities can be evaluated and therefore, vague or sharp transitions can be distinguished objectively.

The last part is the circle at the left side of the phantom (figure 3.3.1 view ”Cavities”) and is a relatively difficult to imagine. As can be seen, within the circle there are eight smaller circular holes, each 0.25 mm deeper than the previous one. In the middle there is a small pin. The back of the circle is flat except

for a small hole in the middle, deep enough for the pin on the front. Two of these units were stacked, creating flat cavities. Each cavity has a specific distance between the two walls to simulate fracture line or joints spaces. With these cavities it was possible to quantify which distance between walls could still be registered after scanning and after the virtual processing . The two units are filled with substances with different radio densities to simulate the difference between fluids as blood in contrast to cartilage.

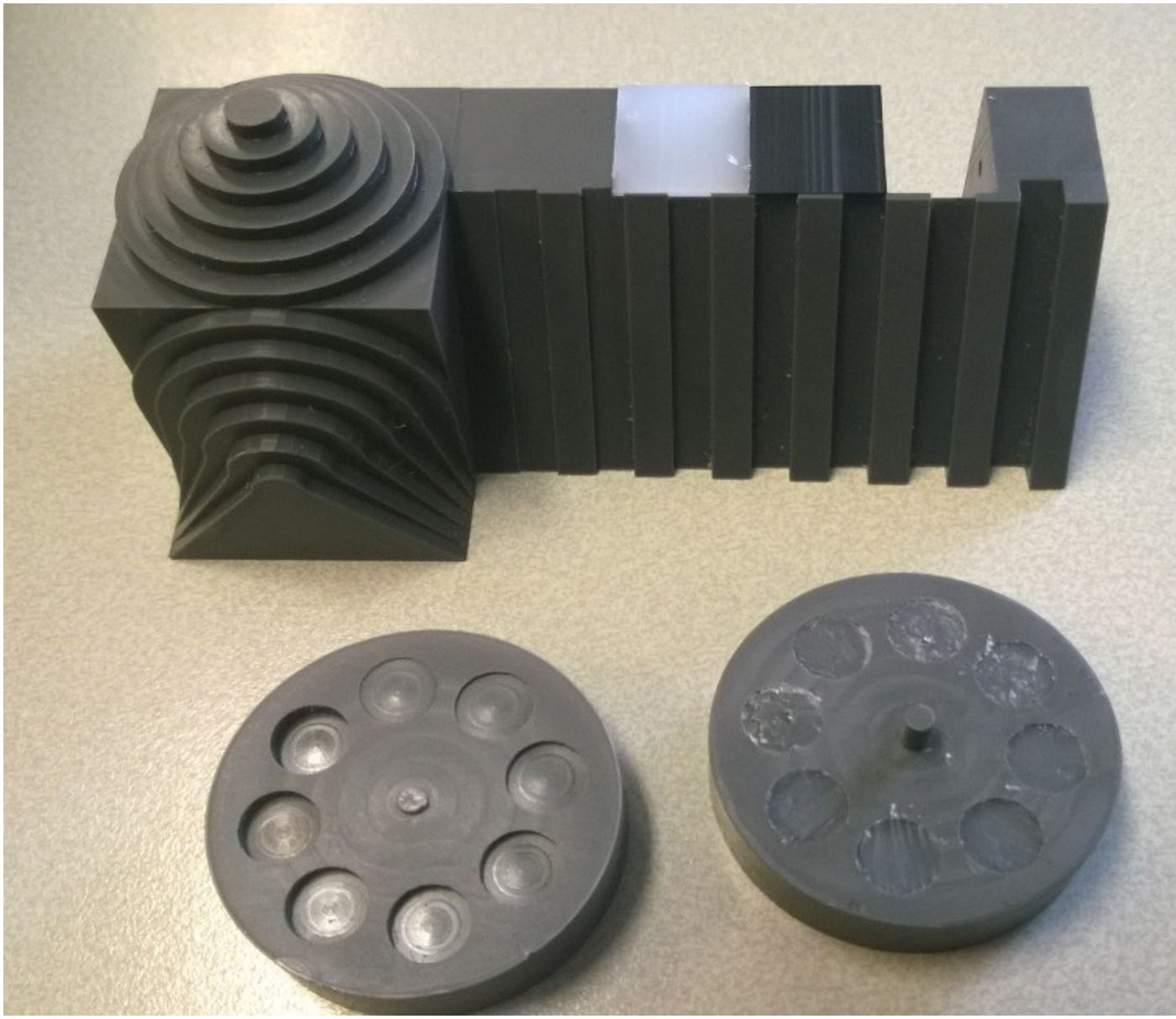

Figure 3.9: 3D image of the phantom disassembled.Click to activate 3D view.

Selecting the proper materials proved to be difficult. For accurate manufacturing , polymers are preferred. However, it is difficult to find polymers with volumetric mass densities close to bone. It is even harder to determine if these have similar radio densities (Hounsfield units) as bone (800 HU spongiosa to 1450 HU cortex), or more extreme, polymers with an decreasing interval of 200 to 300 HU for the blocks. To find the appropriate materials various available materials have been analysed in the CT-scanner, appendix I.This resulted in Polyvinyl chloride (PVC) as main material with around the 950 HU, with Polyvinylidene fluoride (PVDF) around 650 HU and Polyoxymethylene (POM) around 350 HU as materials for the blocks, creating an interval of 300 HU. For filling the cavities silicon glue is selected (ca. 150 HU).

Water is used to compensate for the difference in attenuation within an average shoulder. In the ideal case water and the phantom are contained in a box made of PMMA (Plexiglas), as this material has a similar radiodensity as water. However such a box was not available on short term. Instead, a simple transparent storage container is used. A couple of PMMA blocks are used to centre the phantom. The amount of water can be determined by the water-equivalent diameter, which is around 28 cm for the thorax as defined by J. Menke [32]. The box was 30 cm wide, which meant the water should be around 20 cm high to accommodate the same surface area. The standard 3D shoulder CT-protocol uses a dose modulation algorithm to adjust the tube current according to the attenuation of the body.

This modulation was base around a phantom with a diameter of 32 cm. The average CDTIvol (dose in one cm scan length) from 39 cases was 9.6 mGy* cm. The amount of water was fine-tuned until this CDTIvol was reached in this specific protocol.

The analysed scans were the same as the scans used in the bone study. However, instead of 3D scanning the physical model, the original design of the phantom was used as gold standard for comparison. In addition to the distance deviations, the four parts of the panthom and their characteristics were analysed. The threshold value for the CT-protocols was defined to be lower than the radiodensity of PVC (ca. 950 HU) and higher than PVDF (ca. 650 HU). Models were created from the max tube current protocol with 50 HU interval between the 950 and 650 HU. The resulting models were manually reviewed on their resemblance with the original. The criteria were a minimal average distance deviation and little to no expression of the PVDF block. The same criteria were used for the cbCT, however because no Hounsfield conversion could be made with the cbCT images, each protocol was reviewed separately.

3.3.2 Results

The CT threshold is set on 1700. This setting gave the lowest average distance deviation without only little expression of the PVDF block in the maximal tube current protocol, see table 3.2. The thresholds in the cbCT protocols varied between 23000 and 24000, table 3.3.

Table 3.2: The CT protocol with the maximum tube current, 795 mAs, is used to determine the threshold value. This table showed the resulting distance deviation from different threshold values.

CT protocol 795mAs distance deviations				
Threshold	Min [mm]	Max [mm]	Mean [mm]	RMS [mm]
1750 HU	0	6.323	0.805	0.996
1700 HU	0	6.349	0.654	0.867
1650 HU	0	6.356	0.643	1.007

All the results are shown in table 3.3. All distance deviations were between 0 and 6.33 mm for CT and cbCT. For the CT protocols the average distance deviation slowly increased from 0.77 mm to 1.05 mm between 200 and 75 mAs. In the 50 and 25 mAs protocols the average deviation increased more drastically to 1.45 and 2.11 mm respectively. The average deviations found in the cbCT protocols were from 80 to 5 mAs tube current settings: 0.644, 1.032, 0.844 and 0.936 mm respectively.

In the higher CT protocols every step in the stairs could be distinguished. However, the distinction decreased starting from the 125 mAs protocol and lower. The stairs in cbCT protocols were more prone to artefact due to scattering. This resulted in loss of parts of the steps and indistinct small steps.

Only a small portion of the PVDF block is included in the models created with the CT protocols, especially in contrast to the cbCT protocols. The models from the cbCT protocol included approximately half of thisblock.

3.3.3 Discussion

The four main results are the mean distance deviations, stairs, PVDF block and cavities. The distance deviations verifies if the model is converted to the same dimensions as the original design. In combination with the images (figure 3.3.2) it looks like models are downscaled with at least 0.5 mm. The stairs define which resolution can be (sharply) identified and measured. In the CT protocols this gradually deteriorates with lower dose and in the cbCT protocols identifying the steps becomes harder. The main reason the steps to become unidentifiable is due to the artefacts. The PVDF block is used to define the threshold and in what range the pixel values need to be for differentiation of objects without overlap. In this field the CT protocols are superior. Also visible in figure3.3.3, where a large part of the PVDF block visible. In identifying the cavities the CT protocols are also superior, in exclusion of the 25 mAs protocol.

The CTDIvol dose, is lower in the cbCT compared to the standard CT. The mean distance deviations are promising, however due to artefacts the quality of this scan is inferior. CbCT is more prone to artefact in higher attenuation. In cases with less attenuation, like limbs, the cbCT could show comparable results, but with a lower dose. To investigate this the same scan protocol should be repeated with lower water level to simulated smaller parts of the body.

Some limitations in this research design were the overrepresentation of the attenuation, differences in resolution, conversion of Hounsfield units and lack of vertices in the original design. As described in the method, the level was set to reach a CTDIvol of 9.6 mGy in the standard 3D shoulder protocol with dose modulation. To be precise the CTDIvol was based on the average of 33 cases, but due to some large outliers 9.6 mGy could be an overestimation, as the median was 8.5 mGy. Knowing this error, the overestimation was accepted because it is preferred over an underestimation. Furthermore,

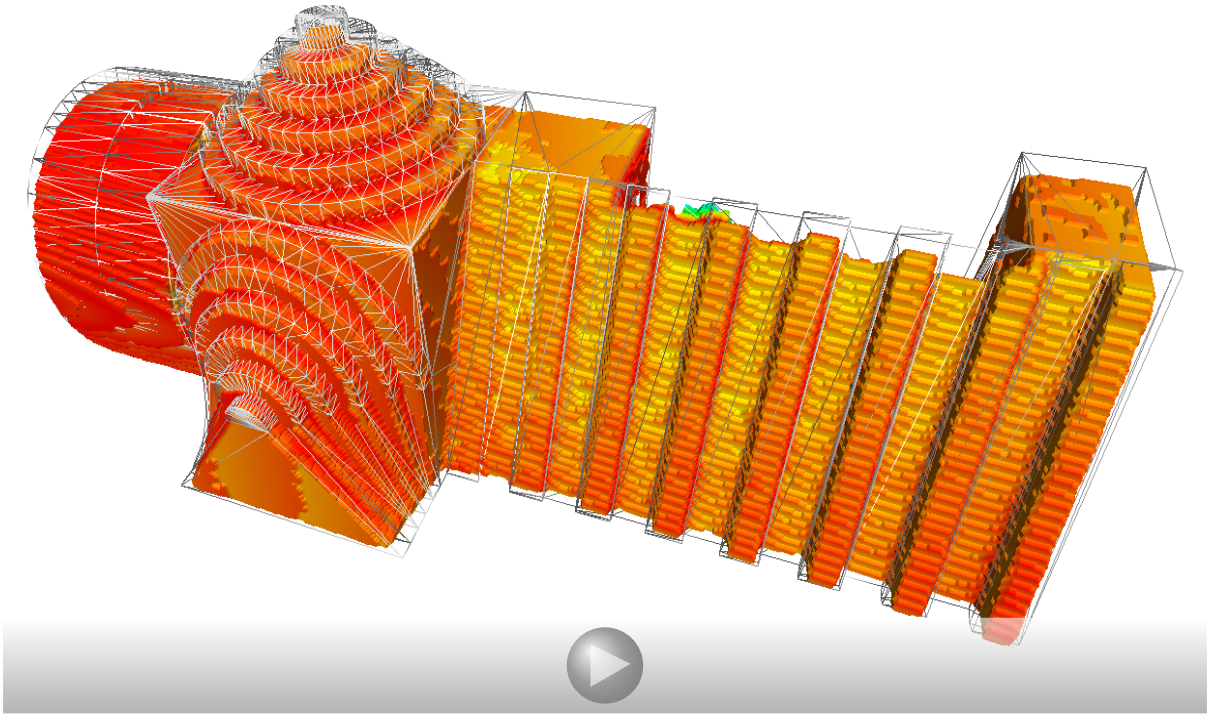

Figure 3.10: Poster image: The colour mapped maximum dose CT model within the ribs of the original design to visualise that the model is smaller than the original. 3D image: 3D model of the maximum dose CT model. Only a small part of the PVDF block is visible. By setting the view to transparent the cavities can be seen.

the phantom itself contained a larger volume of material than a clavicle. This resulted in the scattering over the stairs, which preventeddistinction of the smaller steps.

The used settings in the CT protocol were ideal with a reconstruction diameter of 24 cm and a matrix size of 1024 by 1024, which resulted in a pixel dimension of 0.23 by 0.23 mm. The cbCT did not have many settings to choose from. There were only five settings for tube current: 5, 10, 15, 20 and 80 mAs and a couple of simple reconstruction types and filters. With the standard matrix size of 512 by 512 the pixel dimensions were 0.33 by 0.33 mm and with the lack of complicated filters and reconstruction methods, more noise and artefacts were present. The resolution of this CT protocol was twice as high as the CT protocol in the ClaRP trial, where the reconstruction diameter was doubled to accommodate both clavicles. This results in pixel dimensions of around 0.44 by 0.44 mm. Furthermore, where a standard constant threshold could be set for the CT protocol, this was not possible in the cbCT. This resulted in lack of continuity. Also in clinical applications the exact model shape is not known, which makes it harder to set the right threshold.

Last, both the reconstructed models from the CT and cbCT the design are constructed from vertices, which define the faces. In the distance deviation measurements of the vertices of the reconstructed models were compared with vertices of the design. However, the design is neatly constructed and has only vertices on corners and edges. By using the program Rhinoceros it was possible to increase the number of vertices from 2888 to maximal 12603 vertices. This reduced the problem, but the vertices still were not evenly dispersed and left large surfaces at the bottom without vertices to compare the reconstructed model with. Because this created a constant error between the reconstructed models, the results were still valid for comparison.

This threshold value for the phantom should not be used for bone segmentation, as the material differs. The advice is to acquire this value through a human cadaver study.

Table 3.3: The results from the phantom study. First the eight protocols of the CT are presented with descending tube currents (mAs), followed by four cbCT protocols. First the dose is presented as CTDIvol and the threshold value used to volume render the models. Next two columns state the mean distance deviations and the root mean square. Following columns state the results from the stairs, figure 3.3.1 view "Stairs". First is described which steps are identifiable and secondly the steps that are sharply contoured. The steps are defined in their height in millimetres, increasing with an interval of 0.2 mm. The next column states what percentage of the PVDF triangle block is included in the model. The last two columns give the number of cavities that are identified, first for the cavities filled with water and second the cavities filled with silicon. The decimals state how much of the smallest cavity is visible.

CT protocol [mAs]	CTDIvol [mGy]	Threshold pixel-value	Mean [mm]	RMS [mm]	Stairs identifiable	Stairs sharp	PVDF block [%]	Cavities water	Cavities silicon
200 mAs	13.76	1700	0.769	1.042	0.4	0.6	5	5.4	5.1
175 mAs	12.02	1700	0.776	1.044	0.4	0.6	1	5.1	5.1
150 mAs	10.28	1700	0.792	1.070	0.4	0.6	1	5.1	5.1
125 mAs	8.68	1700	0.854	1.184	0.6	0.8	8	5.1	5.1
100 mAs	6.94	1700	0.888	1.213	0.6	1.2	4	5	5.1
75 mAs	5.21	1700	1.051	1.471	0.8	1.4	5	5	5.1
50 mAs	3.47	1700	1.451	2.014	1.0	1.6	1	5.2	5
25 mAs	1.74	1700	2.108	2.691	1.6	2.0	-1	?	?
cbCT protocol									
80 mAs	15	23500	0.644	1.130	0.4	0.6	30	5.5	4.5
20 mAs	3.47	24000	1.032	1.740	0.8	1.4	40	5.9	4.5
10 mAs	1.88	23500	0.844	1.479	1.0	1.4	70	5.1	3
5 mAs	0.94	23000	0.936	1.464	1.2	1.8	30	5.2	3

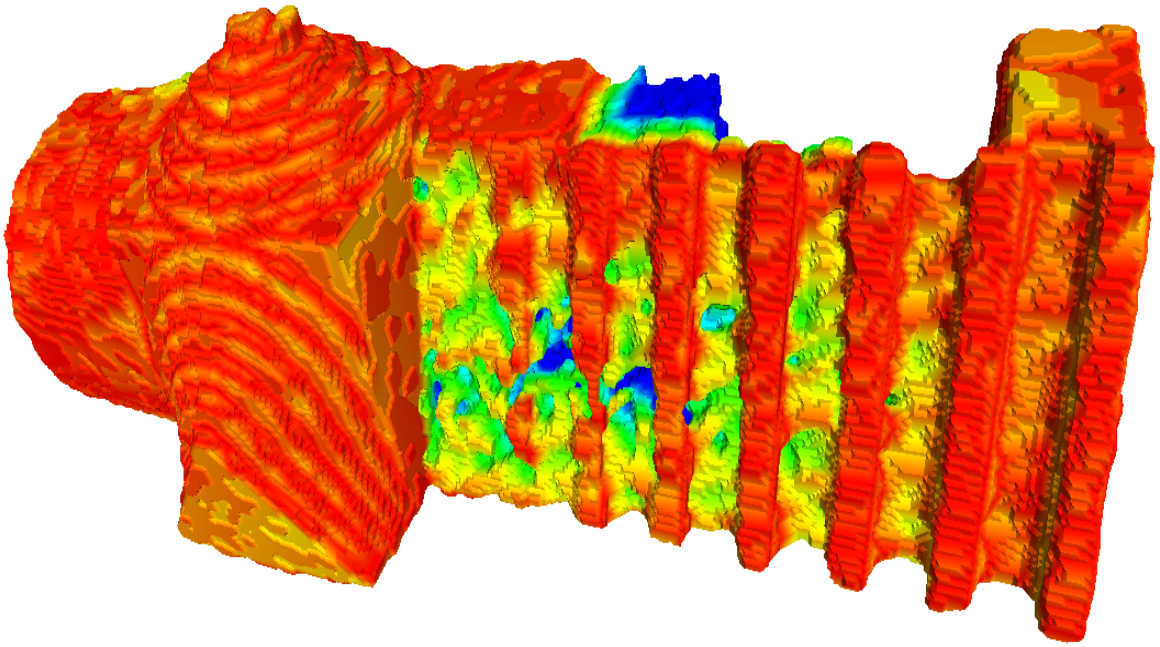

Figure 3.11: Poster image: The colour mapped 10 mAs cbCT model.

Figure 3.12: Poster image: The colour mapped 10 mAs cbCT model. 3D image: the same model, but colours cannot be saved in the 3D model. The artefacts are visible in de stairs and a large portion of the PVDF block is expresed in this model. By setting the view to transparent the cavities can be seen.

Chapter 4

ClaRP: Clinical trial

To further test the clinical relavance of the developed method to precontour osteosynthesis plates, clinical data was needed. To generate this data a clinical study was constructed. As subject of this study the clavicle fracture was chosen, because there was already a good experience with the clavicle fracture through the pilot case (appendix A. Further reasons to choose the clavicle were the fact that in most cases the precontoured plate still had to be bent due to the complex shape of the clavicle, the treatment is a relatively low risk procedure, with small chance of minor complications, which creates a relatively safe environment and they are presented with a relatively constant prevalence.

This chapter reports this clinical study: the ClaRP trial. ClaRP is an acronym for "**Cla**vicle treatment with **R**apid **P**rototyping". The chapter is designed as an isolated article to be submitted to the Journal of Bone and Joint Surgery, ISSN 0021-9355 (Print) 1535-1386 (Electronic). Because the articel is an independent entity some information is repeated from previous chapters in the section "Introduction" and "Materials and Methods".

In this study time reduction was chosen as primary measurement outcome, because this parameter could be objectively quantified and generate useful results within the time span available for this thesis. Furthermore the outcome parameters workflow and screw lenghts are discussed in this version of the article. These last secondary outcome parameters are included for their scientific value in this version. However they are excluded from the final version, because of the difference in target audience.

˙]

Preoperative Osteosynthesis Plate Adjustment using Rapid Prototyping applied to the Clavicle: Clinical Study

R. F. M. van Doremalen, MSc; S.H. van Helden, MD; J.J. Kootstra, MD; E.E.G. Hekman, ir*

Isala; University of Twente
r.f.m.vandoremalen@gmail.com

Abstract

Background: *One method to operatively fix a clavicle fracture is open reduction and internal fixation (ORIF) using plates and screws. For clavicle fractures precontoured osteosynthesis plates are available, however due to the complex shape of the clavicle these plates rarely fit. The plate then has to be bent perioperatively, which is suboptimal in the sterile setting of the operating room. The aim of this study was to test a method in which the plate is preoperatively bent to fit the patients clavicle. The hypothesis was that this will shorten plate handling time and improvement in surgical workflow.*
Methods: *A non-blinded, prospective cohort study was performed. The control group received conventional operative treatment using standard precontoured clavicle locking plates. The intervention group received operative treated using customized plates, which were preoperatively bent. The bending was based on two plastic three dimensional (3D) models, one of the fractured clavicle and a reconstructed model, created by mirroring the contralateral clavicle. These models were created by consecutive CT imaging, segmentation, volume rendering and was subsequently fabricated using rapid prototyping.*
During each operative treatment 3 equivalent surgical proceedings were timed.
Results: *Eight subjects were included in the control group and seven in the intervention group. A plate handling time reduction of 2:04 minutes (p:0.563) was measured, however this time reduction was associated with a lengthened average surgery time of 9:22 minutes (p:0.132). A good integration of the method in the workflow of the surgical team was accomplished.*
Conclusions: *It is possible to implement this rapid prototyping method in fracture treatment. However, no proven added value can be stated. Though surgeon liked the concept of having a plate available with a preoperatively contoured shape, it did not result in a significant time reduction of the procedure. This method may prove its additional value in more complex fracture types.*
Level of Evidence: *Therapeutic Level II*

I. Introduction

Clavicle fractures represent 2.6% of all clinically presented adult fractures, of which 81% is located in the midshaft or diaphysis of the clavicle, the OTA type 15-B fracture [1, 2].

The majority of these fractures are treated with a sling. In case of skin tenting, open fractures, the presence of neurovascular compromise, multiple trauma or fractures with displacement and shortening, operatively fixing the clavicle may be recommended [1, 3, 4, 5, 6]. One method to operatively fix the clavicle is open reduction and internal fixation (ORIF). There are different types of precontoured osteosynthesis plates available for clavicle fracture, however due to the relatively complex shape of the clavicle these plates still rarely fit. To prevent possible complications the plate is bent perioperatively.

The plate then has to be bent perioperatively, which is suboptimal in the sterile setting of the operating room. In a retrospective

*A special thanks to Andre de Vries for his technical support

study between January 2010 and October 2014, at least 36 of the 109 (34%) surgical reports state that the plate was bent perioperatively in Isala (Zwolle, The Netherlands). The aim of this study was to test a method in which the plate is preoperatively bent to fit the patients clavicle through a prospective cohort study. In literature similar techniques are reported for the fractured calcaneus and minimal invasive fixation of clavicle fractures[7, 8]. The hypothesis was that this will shorten plate handling time and improvement in surgical workflow.

II. Methods

I. Study design

This study is an institutional review board-approved, single-center, non-blinded, prospective cohort clinical trial (14.11157, protocol) and is registered with toetsingonline.nl (NL51269.075.14). All subjects provided written informed consent prior to enrollment

Subjects were included from the outpatient clinic of trauma surgery, by the coordinating investigator. All consecutive patients with an acute midshaft clavicle fracture who considered operative treatment were asked to participate. The intervention cohort was started after completion of the control cohort without overlap, to avoid inclusion bias.

The inclusion criteria were equivalent in both groups. However, because of an additional CT scan and preferred symmetry in the preoperative method, some supplementary exclusion criteria are of order. Inclusion criteria:

- Midshaft located clavicle fractures (OTA type 15-B[2])
- Indication for open reduction internal fixation. Indications are displacement and, or shortening, neurovascular compromise, open wound, tenting, or when the patient benefits from quick recovery

Exclusion criteria:

- History of clavicle fractures (intervention group only)
- Pregnancy (intervention group only)
- Age under 14 for control group and under 18 for intervention group

All surgical interventions were performed by trauma surgeons and last year residents with trauma differentiation. No selection of surgeons was made to stay as close as possible to practice as usual. The clinical trial was designed by a technical medicine student and the primary surgeon (S.H. van Helden, MD, Phd). The primary outcome measures were the time differences of three surgical proceedings, the fracture reduction, plate hangling and plate fixation. The secondary outcome measures include the change in workflow, surgeons' experience and screw lengths. The aim of this study was to demonstrate a reduction in plate handling time with preoperative plate bending, furthermore an improved surgical workflow an correlation in the pre- and perioperatively measured screw lengths.

II. Sample size

The sample size of the intervention group was calculated with a power analysis. This analysis was based on the unpaired t-test, with alpha 5% (2-tailed and power 93%). The current plate handling time was estimated by the primary participating surgeon to be 10 minutes with a standard deviation of 2 minutes. The hypotheses was a reduction of time up to 5 minutes with a standard deviation of 2 minutes. It was determined that 5 patients were required in each group. After adding 10% for non-parametrical analysis and taking into account a 10% attrition rate, results in 7 patients to be included.

The sample size of the control group should be at least the size of the intervention group. To avoid bias with overlapping groups, inclusion for the intervention group would not start until treatment of the last subject in the control group was finalized.

III. Preoperative procedure

The whole procedure was conducted within the hospital, without help from a third party. For this study the procedure was performed by the principal investigator, a technical medicine graduate from the University of Twente. The procedure consisted of the following four steps: CT imaging, digital image processing (segmentation and volume rendering), fabrication and plate manipulation. Similar procedures are describe before in literature [9, 10, 11, 12, 13].

First at least 2 days before surgery a CT scan was made (Philips, Brilliance; tube voltage 120kV; tube current 180 mAs, IDose ; scan length 10 - 15 cm; matrix size 1024x1024; reconstruction diameter $\leq$ 500 mm; slice thickness 0.9 mm; increment 0.45 mm). The resulting DICOM (Digital Imaging and Communication in Medicine) files were exported and processed on a separate workstation.

With a program written in MatlabR2014b (The Mathworks Inc. Natick, MA) the clavicles were segmented from the CT images, using the thresholding technique and region growing. The segmentation was subsequently volume rendered, by calculating the isosurface. The result was two 3D surface meshes, which could be exported as stereolithography files (.stl). Successively, the 3D models were further processed in the advanced 3D mesh processing software Meshlab (Visual Computing Lab, Pisa, Italy) to mirror the contralateral clavicle, separate, where necessary, bone fragments from each other and check the model thoroughly before fabrication.

The fabrication was also done with the relatively inexpensive Witbox 3D printer (Bq, Navarra, Spain) in combination with the 3D printing software Cura 15.02.1 (Ultimaking Ltd., Geldermalsen, Netherlands). The models were fabricated within one and half hour using the plastic polylactic acid (PLA) as material. After a small investment of 1700 euro, 1900 US Dollar, for the 3D printer, the costs per clavicle were less than 1 euro/ US Dollar.

Figure 1: *The set up with both models in clay. The fitted plate on the fractured model, outlined on both models. The fracture lines are drawn on the mirrored model.*

With the resulting model of the fractured clavicle and the reconstruction made by mirroring the contralateral clavicle the clavicular plate type and length was selected using unsterile fitting plates. When bending was required a sterile version of the plate was acquired, which would be sterilized before surgery. For bending clay was used to support the models, figure 1. The criteria for the plate were an optimal surface cohesion and a minimum of three screws in the main proximal and distal fragments. Surgical bending irons and pliers were used.

The position of the plate, screw lengths and plan of approach were documented and discussed with the performing surgeon prior to surgery.

IV. Operative intervention

Minimal difference in surgical procedures was aspired between the control and intervention group for comparison. Merely the prior knowledge of the surgeon about the pathology and available osteosynthesis material differed.

In both groups prophylactic antibiotics were given. Under a general anesthetic, the patient was positioned in a beach-chair semi-sitting position. The involved shoulder was prepared and draped, and an oblique incision was made over the fracture site. The fracture site was identified and prepared. The fracture was reduced and temporarily fixed with forceps and/or k-wires. The fracture was fixated with available osteosynthesis plate and screws and the result was check with X-ray before closing the wound.

For comfort a sling was used in the first week after surgery after which small range-of-motion exercises are instructed. Follow up appointments are made two and six weeks after surgery for wound and function evaluation, and further rehabilitation instructions.

V. Measurements

For objective time outcome measurement six moments in surgery are defined, each representing the beginning of the next proceeding, which were timed in both groups for comparison.

T0: Start incision.

T1 (Reduction): The surgeon has exposed the fracture site and starts with the first attempted of fracture reduction with the goal to remain the reduction by means of a forceps or k-wire.

T2 (Plate handling): The moment the surgeon places the plate on the clavicle to assess the compatibility.

T3 (Plate fixation): The first screw is placed.

T4: The last screw is placed.

T5: Last stitch is knotted tight.

The period between T1 and T4 represents the time taken for the fracture treatment and T2-T3 represents the main study parameter, the plate handling. The periods between the other moments are to assess the influence on other proceedings . Three interesting periods in the surgery are measured; the first (T1-T2), second (T2-T3) and last period (T3-T4), that represent the reduction, plate handling and plate fixation respectively. Plate handling may overlap with the reduction period when the contour of the plate is used interim to evaluate the reduction. Or may overlap with the plate fixation period when the plate is used for reduction by fixating the plate to one fragment before reduction with the other. In these cases a combination of periods will be selected for primary study parameter.

The screw lengths were measured on the fractured and mirrored model. The correlation between those measurements and the ultimately place screw lengths was assessed. An estimation of the lengths of the screws perioperatively was made by averaging both to an even number in millimeters and subsequently adding two extra millimeters.

The workflow is assessed by means of a questionnaire for the surgeons. In the questionnaire subjects such as occurred complications and improved orientation are discussed.

VI. Statistical analysis

Continuous variables will be summarized by median (min-max). Categorical variables will be summarized by n(%).

Primary study parameters and additional time parameters:

Time will be recorded. The period between T2 and T3 in time was the primary study parameter. This period will be compared between the two groups using a Mann-Whitney U test. The other recorded periods will be compared similarly.

Secondary study parameter:

Number of errors were registered and experiences will be rated on scales from 1 to 10. Similar to the primary study parameter the significant difference will be proved with a Mann-Withney U test.

Three screw lengths will be measured: from the fractured and mirrored model, and from the planned lengths. These will be compared with the screw length of the locking screws that were ultimately placed peroperatively using a paired t-test.

VII. Source of funding

No source of funding played a role in this study.

III. Results

I. Study Population

Fifteen patients with 15 fractures were entered in the study. Eight patients enrolled in the control group between October and February, age 23 (15-64), of which 3 (38%) patients had a simple fracture (OTA 15B-1) and 5 (62%) had a complex fracture (OTA 15B-2 or -3). Average time between incident and surgery was 12 days (8-16). In the intervention group seven patients were enrolled between March and June, age 40 (32-68), of which 3 (43%) had a simple and 4 (57%) a more complex fracture. Average time between incident and surgery was 16 days (11-30), table 1.

Table 1: *Demographic Data on the Patients*

Parameter	Intervention group	Control group	p-value
Age [median (min-max)]	40y (32-68)	23y (15-64)	0.091
Age fracture [median (min-max)]	16(11-30) days	12(8-16) days	0.061
Sex [M/F]	6/1	5/1	
Fracture type: Simple (B1)	3(43%) cases	3(38%) cases	
Complex (B2)	4(57%)	5(62%)	

Several patients were excluded based on age and one patient was excluded based on a previous clavicle fracture.

II. Surgery Time

The primary study parameter, plate handling (T2-T3) time was not reduced (p-value: 0.643). In the intervention group the proceeding plate handling overlapped with the reduction during surgery, for this reason, as discussed in the method, a combination of these two periods (T1-T3) is a more valid primary study parameter. This combination showed a, nonetheless insignificant, shortening of 2:04 minutes (p-value: 0.563, table 4 and 5). A graphical representation is shown in a boxplot in figure 2.

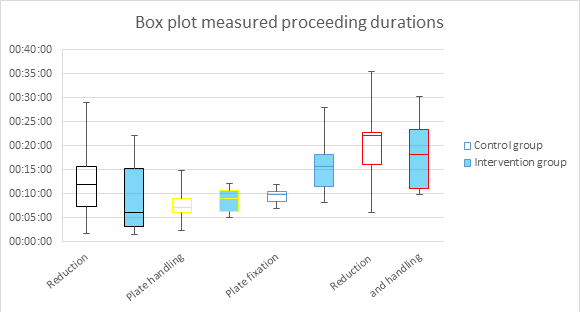

Figure 2: *A boxplot visualizing the measured times for, left to right, reduction (black), plate handling (yellow), plate fixation (blue), and a combination of reduction and plate handling (red). The control group is shown transparent or white and the intervention group the block is light blue.*

Furthermore, the plate fixation time in the intervention group was significantly prolonged with 6:22 minutes (p-value: 0.049) and the overall incision time (T5) was 9:22 minutes longer (p-value: 0.132) in comparison to the control group.

In table 4, it can be seen that the differences are mostly determined by the more complex fractures (OTA type 15-B2 and B3).

III. Experience

No significant differences were found in surgeon's overview and experience, table 2. The principal investigator experienced a time reduction in the preoperative procedure over time. The first cases the procedure took the whole day, while the last few were finished within 4.5 hours.

Table 2: *Surgeon's overview and experience data. (scored from 1 to 10)*

Group [median (min-max)]	Control	Intervention	Significance [P-value]
Overview	6(4-9)	7(4-9)	0.461
Experience	8(7-19)	7.5 (5-9)	0.372

IV. Screw Lengths

In total thirty eight locking screws were placed in the intervention group, table6. On average the measured screw lengths were 1.4 to 1.5 mm shorter than placed locking screws. The 95% coincidence interval ranges within 3 mm.

V. Adverse events

One patient (12.5%) in the control group experienced annoyance of the plate and had it removed. There was one (14%) occurrence of nonunion with infection at the implant site in the intervention group, which was treated by cleaning the wound and fixating the fracture again with a standard plate.

Table 4: *Overview of the different proceedings durations for both groups with its significance.*

Period	Intervention group		Control group		P Value (Asyg. Sig 2-tailed)	
Reduction (T1-T2) [min]	9:33 (SD: 8:12)		12:27 (SD: 8:40)		0.563	
Plate handling (T2-T3) [min]	8:37 (SD: 2:52)		7:48 (SD: 3:47)		0.643	
Plate fixation (T3-T4) [min]	15:52 (SD: 6:37)		9:30 (SD: 1:37)		**0.049**	
Reduct + handl (T1-T3) [min]	18:10 (SD: 8:12)		20:14 (SD: 8:34)		0.563	
Fracture type	B1	B2	B1	B2	B1	B2
Reduction (T1-T2) [min]	9:30 (SD: 11:06)	9:35 (SD: 7:14)	7:36 (SD: 8:22)	15:21 (SD: 8:17)	0.827	0.327
Plate handling (T2-T3) [min]	6:41 (SD: 2:31)	10:04 (SD: 2:25)	6:18 (SD: 4:32)	8:41 (SD: 3:29)	0.827	0.327
Plate fixation (T3-T4) [min]	12:49 (SD: 4:33)	18:09 (SD: 7:35)	9:14 (SD: 2:.4)	9:38 (SD: 1:33)	0.275	0.050
Fract treatment (T1-T4) [min]	34:03 (SD: 9:45)		29:44 (SD: 8:21)		0.355	
Incision time (T5) [min]	1:02:07 (SD: 12:.7)		52:46 (SD: 13:37)		0.132	

Table 5: *Statistical difference of the intervention compared to the control group.*

Period	Mean Difference	Std. Error Difference	95% CI of the Difference	
			Lower	Upper
Reduction (T1-T2) [min]	0:02:53	0:04:21	-0:06:32	0:12:19
Plate handling (T2-T3) [min]	-0:00:49	0:01:43	-0:04:33	0:02:55
Plate fixation (T3-T4) [min]	-0:06:22	0:02:34	-0:12:31	-0:00:14
Reduction plus plate handling (T1-T3) [min]	0:02:04	0:04:20	-0:07:18	0:11:26
Wh ole fracture treatment (T1-T4)	-0:04:18	0:04:43	-0:14:36	0:05:59
Incision time (T5) [min]	-0:09:22	0:05:55	-0:22:16	0:03:31

Table 6: *Statistical comparison of the difference in length between the operatively placed screws and the preoperative measured screws. Measurements were based on the mirrored and fractured model. For the fractured model the difference in length was corrected (Diff corr) to objectively assess the deviations from the perioperatively measured lengths.*

	Paired Differences					Significance
		Standard	Standard	95% CI of the Difference		
	Mean	deviation	error	Lower	Upper	(2-tailed)
Mirrored	1.42	2.71	0.44	0.53	2.31	0.003
Fracture	1.46	2.20	0.36	0.74	2.18	0.000
Fracture+1.5	-0.04	2.20	0.36	**-0.76**	**0.68**	**0.913**

IV. Discussion

I. Time measurements

The moments in surgery were selected with the aim to intercept the proceedings specific to the intervention of fixating the clavicle fracture. The proceedings opening and closing the patient, preparing the bone and evaluating the results by means of x-ray are taken out of the equation in this manner. What remains are the treatment specific proceedings, differentiated into the reduction of the fracture, plate handling and plate fixation. Although a lot of thought went into picking the right moments, each of them had its flaws.

T1 was the moment where the surgeon starts to manipulate the bone fragments, with the goal of finding the correct reduction and holding it in this position. The transition between preparing the bone and starting the reduction was a relatively vague moment. It can happen that after initiating the reduction some parts still needed to be prepared. Sometimes the reduction could be continued, other times it had to start from the beginning, which made this moment hard to recognize. For this reason the researcher was present to measure the time frames himself to avoid interobserver variability.

T2 was the moment the plate touched the bone, to indicate the start of the plate handling. In some cases when the plate touched the bond for the first the instruments used to temporarily hold the reduction in place obstructed the placement of the plate and had to be moved. This started the plate handling period, was technically not a part of this period and created an error in both groups. As mentioned was the plate used to evaluate the reduction the intervention group. This action initiated the plate handling period, while the reduction was not yet finished. This resulted in a misrepresentation: the reduction was shortened and the plate handling time lengthened. For this reason the two periods combined were also analyzed, table 4 and 5.

For T3 the moment of the first screw was fixated in the plate was chosen. It was known that by doing so the drilling of the hole, measuring the screw length and selection and fixation of the screw was included within the plate handling period. This is a constant error was accepted to create a clear measurement moment. It appeared in both groups and took around two to three minutes.

T4, like T3, had a clear indication in moment of time. The period between these two was initially inserted to include the effect on it when the reduction was done based on the plate. In this case the first screw would be placed before the reduction was completed. Furthermore, it was hypnotized that predetermining the screw lengths would shorten this period. However, in the end all screw lengths were still measured perioperatively. The end result of a significant lengthening of 7:12 minutes could not be appointed to any apparent cause.

T5 was the closing of the patient, indicating the end of the incision time. The average incision time in the intervention group was 9 minutes 22 longer. This was an additional

5 minutes above the measured difference in the fracture treatment period (T1-T4). This is probably due to the fact that the days between trauma and surgery were on average 4.5 days longer (12 vs 16.5 days). In this time more callus could be formed which would increase the time needed to open the patient and prepare the fracture. These proceedings were before T1, so that the callus formation would have had no effect time measurement T1 to T4.

II. Surgeons' experience

The questionnaires, filled in at the end of surgery, were inconclusive. The variation in surgeons performance, among others, made this tool useless. The principal investigator was present during all cases and discussed the procedure with the surgeon prior to and after surgery. This lead to a less objective summary of beneficial experiences.

First, a preoperative benefit is that the documentation provides an extensive graphical representation the present pathology and instructions about the material placement. Also, having the models present helps to give a spatial understanding of the position, size and shape of the fragments. This may help in planning the incision and preparing the bone without disconnecting the fragments from blood supply. In the intervention group no small bone fragments were removed, in contrast to the control group.

Second, having a plate with a curvature resembling the one of the clavicle is useful for testing the obtained reduction.

In the end no time reduction in the procedure could be indicated. Though the surgeons liked the concept of having a plate available with a preoperatively contoured shape.

III. Preoperative workhours

In research setting the preoperative planning took a relative long time, due to a learning curve and inefficient set up. Image acquisition, processing and fabrication , and plate manipulation each took place in a different setting and location. Furthermore, many proceedings had to be figured out along the way and double checked for preventing possible errors to occur.

IV. Intersurgeon variability

Initially the protocol stated that all the interventions were to be performed by one or two involved surgeons. Unfortunately, this set-up was not feasible. This would conflict with the schooling of the present residents. Planning the subjects in such manner already proved to be problematic in the control group. For this reason the choice was made to change to a random surgeon, selected through the daily course of events.

The scientific benefit now was that the research population a more accurate representation of the reality was and therefore comparable with standard circumstances. Besides that, because each surgeon participated maximal two times in the intervention group, their learning effect was minimal. Unfortunately, the intersurgeon variability influenced the measurements more than anticipated. For example one surgeon, who only participated in the control group, was for this specific operation on average 12 and a half minute (SE: 11.255) faster than the other surgeons. This was calculated in a retrospective study over the years 2012 and 2013 . Furthermore, as established before, it influenced the assessment of their experiences in the workflow questionnaire.

V. Learning curve

Among the surgeons no learning curve was witnessed due to the intersurgeon variability. With the planner or investigator, on the contrary, an apparent learning curve was present. Not only in the planning itself, which took big steps in efficiency and duration. Also during surgery steadily a number of things were learned, such as the necessity of trust from the surgeon and a few considerations in the preparations.

The main issue was trust. In case of simple fractures reduction on the plate should be

possible, but due to lack of trust in the curvature of the plate, the surgeon still preferred a temporarily reduction with forceps before fixation. After this reduction the plate curvature would coincide with the instruments used for the temporal fixation. This meant that during the adjustment of the plate the temporal reduction had to be taken into account. For this the planner had to learn the restrictions of this proceeding and the preferences of each surgeon. If the temporal reduction was not performed as planned, the plate would again coincide with the used instruments. For this reason, the surgeon also had to trust the planning of the reduction for the procedure to be a success.

In the end it proved to be important for the planner to be present perioperatively to assess the preparation of the bone and placement of the plate. Being involved in the planning proved to be an advantage in evaluating the reduction and position of the material.

VI. Priorities

One can roughly divide fracture surgeries in extra-articular and intra-articular fractures. Anatomic reduction and fixation are necessary in the second group. Clavicle fractures are extra-articular shaft fractures and therefore secondary bone healing with non-anatomical reduction will also result in a good functional result. Whereas in intra-articular fractures perfect alignment is aspired to prevent complications like loss of function, pain or damage to a joint.

Because non-anatomical reduction is accepted in extra-articular fractures the focus in these surgeries lies more on speed and fracture compression. With this mindset the control group is treated. The intervention group however, a perfect reduction was needed to accommodate the preoperative planning and the precontoured plate. This would cost extra time and it is suspected that this accounts for the elongation of the surgeries in the intervention group. To support this hypothesis, the study should be repeated with an extra-articular fracture type.

VII. Screw lengths

In determining the screw length it is important that the thread is through both cortex layers and the point does not protrude too much on the other side. Two to four millimeters is considered acceptable according to the expert opinion of the primary surgeon.

The 95% confidence interval range was within 3 mm and on average 1.5 mm to short. By adding 3 to 4 mm to the measured length the length should stay within the safe limits. To support this claim, the mean difference was added to the fractured model, called âĂIJFracture+1.5âĂİ in table 6. The result had a p-value of 0.913, which concludes that it is not significantly similar.

For this study the placed screws were considered as the gold standard. However the perioperative measurements were not accurate. For accurate assessment an postoperative CT scan should be made to assess the screw lengths. The attempt is made to assess the screw lengths through blinded postoperative X-ray images of both groups by the primary surgeon. However X-ray images deemed unsuited for this task.

VIII. Utility assessment

Do the benefits outweigh the extra CT scan and preoperative workhours? This study indicates that the surgical intervention will not be shortened, however, the new procedure may improve the workflow for the surgical team. To objectively quantify the improved reduction as well as the screw placement, postoperative CT scans are needed. To assess improved patient outcome a larger sample size with a follow up of at least one to two years per patient is required. In summary, the resulting benefits are subjective and do not prove to be an additional value, at least not in contrast to the need of an extra CT scan and the efforts accompanying the preoperative planning.

V. Conclusion

A preoperatively fitted plate showed subjective benefits in the surgical workflow. Unfortunately, it does not outweigh the extra CT scan end effort that goes into the preoperatieve preparation. No significant surgical time reduction could be demonstrated.

References

[1] F. Postacchini, S. Gumina, P. De Santis, and F. Albo, "Epidemiology of clavicle fractures," *Journal of Shoulder and Elbow Surgery*, vol. 11, no. 5, pp. 452–456, 2002.

[2] M. JL, S. TF, A. J, B. JS, C. W, D. TA, P. L, S. MS, Z. B, H. B, and A. L., "Fracture and dislocation classification compendium - 2007: Orthopaedic Trauma Association classification, database and outcomes committee.," *Journal of Orthopaedic Trauma*, vol. 21, pp. 72–74, 2007.

[3] K. Virtanen, V. Remes, A. Malmivaara, and M. Paavola, "Treatment of clavicle fractures : systematic review," *Suomen Ortopedia ja Traumatologia*, vol. 32, pp. 134–139, 2007.

[4] Y. Melenevsky, C. M. Yablon, A. Ramappa, and M. G. Hochman, "Clavicle and acromioclavicular joint injuries: a review of imaging, treatment, and complications.," *Skeletal radiology*, vol. 40, pp. 831–42, July 2011.

[5] F. J. G. Wijdicks, P. J. Millett, R. M. Houwert, O. a. J. Van Der Meijden, and E. J. M. M. Verleisdonk, "Systematic review of the complications of plate fixation of clavicle fractures," *Archives of Orthopaedic and Trauma Surgery*, vol. 132, no. 5, pp. 617–625, 2012.

[6] P. L. Althausen, S. Shannon, M. Lu, T. J. O'Mara, and T. J. Bray, "Clinical and financial comparison of operative and nonoperative treatment of displaced clavicle fractures.," *Journal of shoulder and elbow surgery / American Shoulder and Elbow Surgeons ... [et al.]*, vol. 22, pp. 608–11, May 2013.

[7] K. J. Chung, D. Y. Hong, Y. T. Kim, I. Yang, Y. W. Park, and H. N. Kim, "Preshaping Plates for Minimally Invasive Fixation of Calcaneal Fractures Using a Real-Size 3D-Printed Model as a Preoperative and Intraoperative Tool," *Foot & Ankle International*, vol. 35, no. 11, pp. 1231–1236, 2014.

[8] H.-S. Jeong, K.-J. Park, K.-M. Kil, S. Chong, H.-J. Eun, T.-S. Lee, and J.-P. Lee, "Minimally invasive plate osteosynthesis using 3D Printing for shaft fractures of clavicles: technical note," *Archives of Orthopaedic and Trauma Surgery*, vol. 134, no. 11, pp. 1551–1555, 2014.

[9] G. a. Brown, K. Firoozbakhsh, T. a. DeCoster, J. R. Reyna, and M. Moneim, "Rapid prototyping: the future of trauma surgery?," *The Journal of bone and joint surgery. American volume*, vol. 85-A Suppl, pp. 49–55, 2003.

[10] F. Rengier, A. Mehndiratta, H. Von Tengg-Kobligk, C. M. Zechmann, R. Unterhinninghofen, H. U. Kauczor, and F. L. Giesel, "3D printing based on imaging data: Review of medical applications," *International Journal of Computer Assisted Radiology and Surgery*, vol. 5, no. 4, pp. 335–341, 2010.

[11] V. Bagaria, S. Deshpande, D. D. Rasalkar, A. Kuthe, and B. K. Paunipagar, "Use of rapid prototyping and three-dimensional reconstruction modeling in the management of complex fractures.," *European journal of radiology*, vol. 80, pp. 814–20, Dec. 2011.

[12] G. Biglino, S. Schievano, and A. M. Taylor, "The Use of Rapid Prototyping in Clinical Applications," in *Advanced Applications of Rapid Prototyping Technology in Modern Engineering* (M. Hoque, ed.), InTech, 2011.

[13] M. Frame and J. S. Huntley, "Rapid prototyping in orthopaedic surgery: a user's guide.," *TheScientificWorldJournal*, vol. 2012, pp. 1–7, Jan. 2012.

Chapter 5

Discussion

5.1 Rapid prototyping in fracture treatment

From the ClaRP trial it can be said that this method does not improve clavicle fracture treatment, because it is extra articular fracture. The goal of the treatment is not a perfect anatomical reduction but, only a rigid reduction with fracture compression. The question remains whether the method is applicable, and if so, advantageous in more challenging cases. Therefore, concurrent with the ClaRP trial cases, the method was tried on other, more challenging fracture types and a inter-articular fracture, a distal intra articular humerus fracture, a pelvic fracture and a rotation malunion of a radius. Short descriptions of these cases can be found in appendix J.

In these cases perfect reductions were aspired, or as often in pelvis fractures, the fracture was difficult to reach with a minimal view. In these cases the 3D modeling and a plastic replica showed an added value to the process to be able to produce a more accurate preoperative planning. The similarity between these cases is that there was a relatively high risk of complications and an accurate reduction was aspired for optimal results.

5.2 Tactical hospital implementation

The ClaRP trial was meant to give deeper insight into the possibilities of the use of rapid prototyping in fracture treatment and to clarify the technical, practical and organizational difficulties and limitations in daily practice. The research setting was not ideal and for practical implementation a more central location is desired. To investigate this issue literature was consulted and several specialists within and outside Isala were interviewed. Multiple events were attended on this matter and implementations in other hospitals were reviewed, like the 3D lab in UMC Radboud and UMCG or the Papid Pro conference.

With the created network, from for instance the Rapid Pro conference, a meeting was proposed and organized in Isala to share knowledge concerning this issue and to brainstorm for future implementation. At this meeting a specialist, technical physicians and medical technicians from UMCG, Isala and Gelre hospital were present. In summary, a couple of conclusions could be drawn from this meeting. For a broad and tactical implementation of a 3D platform within a hospital the medical technology department would be ideal. This department already facilitates the medical departments on the technical aspect, which means the knowledge and the network is present. From experience it became apparent that a main application is needed at first to get such platform started, an application which contributes a constant demand from the platform. From here on through good promotion and education more applications at different departments can be retrieved. With every application it is important that someone from the clinical field, a physician or specialist, is motivated and enthusiastic for a thorough implementation.

Furthermore, the discussion was continued about the discrepancies between open source and commercial services. Whereas open source is free and does not hold back development, commercial services come with a price but provide a validated and certified product and offer support. This equally applies to rapid prototyping and software.

5.3 Other applications

In this thesis the objective was to create a patient specific plate. In a broader sense this is a patient specific tool or design. The main role of a 3D platform is virtual diagnostics or planning. In virtual planning a relatively accurate treatment can be designed, however, in the transition between planning and execution most accuracy may be lost. To prevent this loss of accuracy a patient specific tool is needed. In this case a patient specific plate was created, but other methods are possible and available. Options are navigation (e.g. Brainlab in brain surgery), robotics (e.g. Da Vinci system or laser eye

surgery), surgical templates, guides or jigs used in jaw reconstruction or joint prosthesis placement (e.g. Materialise, VISIONAIRE ^{TM}, MyKnee, Zimmer, etc.). These options can be used separately or combined.

These methods are applied in cases where accuracy and perfection is essential. In most trauma surgery cases accuracy and perfection is subordinated to speed and acting quickly. Most fractures, as the midshaft clavicle fracture, remodel efficiently even when the reduction is not optimal, thus the clinical relevance of improving the treatment is minimal. However this method could provide good prospectives in cases as pelvis fractures, correction osteotomies and interarticular fractures.

Chapter 6

Conclusion

It is possible to integrate rapid prototyping in trauma surgery when good arrangements are made with medical imaging, medical technology and the central sterilisation administration. The application of rapid prototyping, as shown in the ClaRP trial, contributes no significant time reduction. The added value of rapid prototyping is the direction of accuracy and quality. It can give surgeons the opportunity to properly prepare for surgery, as some form of rehearsal. Improved quality and accuracy could not be measured on such short term.

References

[1] D.-G. Ahn, J.-Y. Lee, and D.-Y. Yang, "Rapid Prototyping and Reverse Engineering Application for Orthopedic Surgery planning," *Journal of Mechanical Science an Technology*, vol. 20, no. 1, pp. 18–28, 2006.

[2] K. J. Chung, D. Y. Hong, Y. T. Kim, I. Yang, Y. W. Park, and H. N. Kim, "Preshaping Plates for Minimally Invasive Fixation of Calcaneal Fractures Using a Real-Size 3D-Printed Model as a Preoperative and Intraoperative Tool," *Foot & Ankle International*, vol. 35, no. 11, pp. 1231–1236, 2014.

[3] H.-S. Jeong, K.-J. Park, K.-M. Kil, S. Chong, H.-J. Eun, T.-S. Lee, and J.-P. Lee, "Minimally invasive plate osteosynthesis using 3D Printing for shaft fractures of clavicles: technical note," *Archives of Orthopaedic and Trauma Surgery*, vol. 134, no. 11, pp. 1551–1555, 2014.

[4] V. Bagaria, S. Deshpande, D. D. Rasalkar, A. Kuthe, and B. K. Paunipagar, "Use of rapid prototyping and three-dimensional reconstruction modeling in the management of complex fractures.," *European journal of radiology*, vol. 80, pp. 814–20, Dec. 2011.

[5] F. Qiao, D. Li, Z. Jin, Y. Gao, T. Zhou, J. He, and L. Cheng, "Application of 3D printed customized external fixator in fracture reduction," *Injury, Int. J. Care Injured*, vol. 46, no. 6, pp. 1150–5, 2015.

[6] J. C. Yang, X. Y. Ma, J. Lin, Z. H. Wu, K. Zhang, and Q. S. Yin, "Personalised modified osteotomy using computer-aided design-rapid prototyping to correct thoracic deformities," *International Orthopaedics*, vol. 35, no. 12, pp. 1827–1832, 2011.

[7] G. a. Brown, K. Firoozbakhsh, T. a. DeCoster, J. R. Reyna, and M. Moneim, "Rapid prototyping: the future of trauma surgery?," *The Journal of bone and joint surgery. American volume*, vol. 85-A Suppl, pp. 49–55, 2003.

[8] Z. a. Starosolski, J. H. Kan, S. D. Rosenfeld, R. Krishnamurthy, and A. Annapragada, "Application of 3-D printing (rapid prototyping) for creating physical models of pediatric orthopedic disorders," *Pediatric Radiology*, vol. 44, no. 2, pp. 216–221, 2014.

[9] R. a. Watson, "A low-cost surgical application of additive fabrication," *Journal of Surgical Education*, vol. 71, no. 1, pp. 14–17, 2014.

[10] M. Olsen, D. D. Naudie, M. R. Edwards, M. E. Sellan, R. W. McCalden, and E. H. Schemitsch, "Evaluation of a patient specific femoral alignment guide for hip resurfacing," *Journal of Arthroplasty*, vol. 29, no. 3, pp. 590–595, 2014.

[11] G. Biglino, S. Schievano, and A. M. Taylor, "The Use of Rapid Prototyping in Clinical Applications," in *Advanced Applications of Rapid Prototyping Technology in Modern Engineering* (M. Hoque, ed.), InTech, 2011.

[12] M. Frame and J. S. Huntley, "Rapid prototyping in orthopaedic surgery: a user's guide.," *TheScientificWorldJournal*, vol. 2012, pp. 1–7, Jan. 2012.

[13] F. Rengier, A. Mehndiratta, H. Von Tengg-Kobligk, C. M. Zechmann, R. Unterhinninghofen, H. U. Kauczor, and F. L. Giesel, "3D printing based on imaging data: Review of medical applications," *International Journal of Computer Assisted Radiology and Surgery*, vol. 5, no. 4, pp. 335–341, 2010.

[14] R. Haaker and W. Konerman, "Computer and Template Assisted Orthopedic Surgery," tech. rep., 2013.

[15] T. J. Maal, *3D Stere ophotogrammetry in Oral and Maxillofacial Surgery*. PhD thesis, UMC Radboud, 2012.

[16] R. H. Schepers, G. M. Raghoebar, A. Vissink, M. W. Stenekes, J. Kraeima, J. L. Roodenburg, H. Reintsema, and M. J. Witjes, "Accuracy of fibula reconstruction using patient-specific CAD/-CAM reconstruction plates and dental implants: A new modality for functional reconstruction of mandibular defects," *Journal of Cranio-Maxillofacial Surgery*, vol. 43, no. 5, pp. 649–657, 2015.

[17] J. G. G. Dobbe, J. C. Vroemen, S. D. Strackee, and G. J. Streekstra, "Patient-tailored plate for bone fixation and accurate 3D positioning in corrective osteotomy," *Medical and Biological Engineering and Computing*, vol. 51, no. 1-2, pp. 19–27, 2013.

[18] J. G. G. Dobbe, J. C. Vroemen, S. D. Strackee, and G. J. Streekstra, "Patient-tailored plate for bone fixation and accurate 3D positioning in corrective osteotomy," *Medical and Biological Engineering and Computing*, vol. 51, no. 1-2, pp. 19–27, 2013.

[19] B. Kleinhenz P and M. Stern S, "http://emedicine.medscape.com/article/92429-overview : Clavicle fractures," December 2014.

[20] M. JL, S. TF, A. J, B. JS, C. W, D. TA, P. L, S. MS, Z. B, H. B, and A. L., "Fracture and dislocation classification compendium - 2007: Orthopaedic Trauma Association classification, database and outcomes committee.," *Journal of Orthopaedic Trauma*, vol. 21, pp. 72–74, 2007.

[21] F. Postacchini, S. Gumina, P. De Santis, and F. Albo, "Epidemiology of clavicle fractures," *Journal of Shoulder and Elbow Surgery*, vol. 11, no. 5, pp. 452–456, 2002.

[22] Y. Melenevsky, C. M. Yablon, A. Ramappa, and M. G. Hochman, "Clavicle and acromioclavicular joint injuries: a review of imaging, treatment, and complications.," *Skeletal radiology*, vol. 40, pp. 831–42, July 2011.

[23] F. J. G. Wijdicks, P. J. Millett, R. M. Houwert, O. a. J. Van Der Meijden, and E. J. M. M. Verleisdonk, "Systematic review of the complications of plate fixation of clavicle fractures," *Archives of Orthopaedic and Trauma Surgery*, vol. 132, no. 5, pp. 617–625, 2012.

[24] P. L. Althausen, S. Shannon, M. Lu, T. J. O'Mara, and T. J. Bray, "Clinical and financial comparison of operative and nonoperative treatment of displaced clavicle fractures.," *Journal of shoulder and elbow surgery / American Shoulder and Elbow Surgeons ... [et al.]*, vol. 22, pp. 608–11, May 2013.

[25] C. Vanbeek, K. J. Boselli, E. R. Cadet, C. S. Ahmad, and W. N. Levine, "Precontoured plating of clavicle fractures: Decreased hardware-related complications?," *Clinical Orthopaedics and Related Research*, vol. 469, no. 12, pp. 3337–3343, 2011.

[26] K. J. Virtanen, A. O. V. Malmivaara, V. M. Remes, and M. P. Paavola, "Operative and nonoperative treatment of clavicle fractures in adults," *Acta Orthopaedica*, vol. 83, no. 1, pp. 65–73, 2012.

[27] R. C. McKee, D. B. Whelan, E. H. Schemitsch, and M. D. McKee, "Operative Versus Nonoperative Care of Displaced Midshaft Clavicular Fractures: A Meta-Analysis of Randomized Clinical Trials," *The Journal of Bone and Joint Surgery (American)*, vol. 94, no. 8, p. 675, 2012.

[28] M. Lenza, R. Buchbinder, R. Johnston, J. Belloti, and F. Faloppa, "Surgical versus conservative interventions for treating fractures of the middle third of the clavicle," *Clinical Orthopaedics and Related Research*, vol. 472, no. 9, pp. 2579–2585, 2013.

[29] G. D. Liu, S. L. Tong, S. Ou, L. S. Zhou, J. Fei, G. X. Nan, and J. W. Gu, "Operative versus non-operative treatment for clavicle fracture: A meta-analysis," *International Orthopaedics*, vol. 37, no. 8, pp. 1495–1500, 2013.

[30] C. H. Rehn, M. Kirkegaard, B. Viberg, and M. S. Larsen, "Operative versus nonoperative treatment of displaced midshaft clavicle fractures in adults: a systematic review," *European Journal of Orthopaedic Surgery and Traumatology*, vol. 24, pp. :1047–1053, 2013.

[31] J. Xu, L. Xu, W. Xu, Y. Gu, and J. Xu, "Operative versus nonoperative treatment in the management of midshaft clavicular fractures: a meta-analysis of randomized controlled trials.," *Journal of shoulder and elbow surgery*, vol. 23, no. 2, pp. 173–81, 2014.

[32] J. Menke, "Comparison of different body size parameters for individual dose adaptation in body CT of adults.," *Radiology*, vol. 236, no. 2, pp. 565–571, 2005.

Appendix A

Case report pilot study

A.1 Introduction

Clavicle fractures represent 2.6% of all clinically presented adult fractures, of which 81% are located in the midshaft or diaphysis of the clavicle, the OTA type 15-B fracture8, 10. The majority of these fractures are treated with a sling. In cases where the fracture shows skin tenting, open fractures, the presence of neurovascular compromise, multiple trauma or fractures with displacement and shortening, surgical treatment may be recommended1, 9, 12, 13, 14. Between January 2010 and October 2014, 110 patients had open reposition and internal fixation of their type 15-B fracture in the Isala (Zwolle, The Netherlands). According to the surgery reports, the used plate did not fit the broken clavicle in 37 cases (34%). It had to be altered by bending perioperatively or exchanging by another plate. In four cases, (4%) the lateral part of the plate was placed medially, and the other way around. The alteration process takes time and the resulting quality of alteration may differ between surgeons and surgeries. Preoperative planning is a manner in which to improve current efficiency and workflow in open reposition and internal fixation procedures. The perioperative alteration process can be avoided by performing the osteosynthetic plate selection and adjustment preoperatively. This could be done by constructing a physical three-dimensional model of the fractured clavicle and/or the mirrored version of the contralateral clavicle. In this manner, the plate can be adjusted preoperatively to fit the curvature of the (modelled) clavicle. The literature reports a similar technique for the fractured calcaneus and minimal invasive fixation of clavicle fractures4, 7. In this case we report the repair of a clavicle pseudarthrosis supported by low budget, in hospital, rapid prototyping. Keywords: Clavicle, Rapid Prototyping, 3D printing, Fracture, Pseudarthrosis

A.2 Case report

A 27-year-old woman on a bicycle, was hit by a car travelling at an estimated speed of 40 km/h. This resulted in a head injury and a fractured clavicle and tibia. The head injury had no serious effects, the clavicle was treated conservatively and the fractured tibia was fixed intramedullary. By mere stabilization of the shoulder with a sling the clavicle fracture did not consolidate and after a year she still experienced limited function of her shoulder. An attempt to treat the fracture with a bone growth stimulator was futile and after seventeen months the pseudarthrosis of the clavicle fracture was planned for surgical fixation by means of an open reposition and internal fixation.

The prolonged period of time resulted in extensive remodeling of the bone around the fracture site. This has resulted in bulky fracture lines and shortening of the clavicle, due to callus formation and bone resorption respectively (figure 1).

A CT scan of both clavicles was made. From this scan, using the mathematical software Matlab (The Mathworks Inc., Natick, MA), the clavicles were segmented, converted into 3D surface mesh models (figure 2) and exported as stereolithography files (.stl). Thereafter, the exported models were processed in the program Meshlab (Visual Computing Lab, Pisa, Italy). Some example processing steps are, mirroring the contralateral clavicle and separating the fragments. The result was one representative model of the fractured clavicle and one of the mirrored contralateral clavicle. The next step was to create physical models by means of a rapid prototyping technique (figure 1). In this case the plastic models were created out of PLA (polylactic acid) by means of fused deposition modeling, using a low-budget 3D-printer, the bq Witbox (figure 3). This printing process has been described in detail before 2, 3, 6, 11. Two models were available for fitting the plate, the fractured clavicle and the mirrored contralateral clavicle. Since the majority of the patients has symmetrical clavicles5, and in the present case remodeling created an unrealistic representation of the bone structure, the mirrored contralateral reconstruction was used as a guide for the curvature of the plate (figure 4). Furthermore, the same tools as used in surgery were used to assess the curvature of the plate before sterilization.

With these models, the type of plate and the optimal location on the clavicle were predetermined. Several different available plates were tested that there was a maximum bone to plate contact, and three screws on the medial and lateral fragment were able to penetrate both cortical layers of the clavicle. If a standard plate had met these requirements, a sterile version could have been used during surgery. In the present case the targeted plate was bent to fit the models and resterilized for surgical use.

As a result, the surgery was technically a success. This entails that no surgery time was spent on altering the osteosynthetic plate and the clavicle was reconstructed on the curvature of the plate. Demineralized bone matrix was used to fill the gap in the fracture caused by the remodeling of the bone. The accumulated time it took to prepare for surgery in this single case was approximately 4 hours.

Eleven months follow-up showed no pain or irritations and consolidation of the fracture (figure 5).

A.3 Discussion

This case shows that improvements can be made in the workflow of the conventional operative procedure. Usually a plate is selected based on the repositioned fracture perioperatively. Now, with a better preoperative orientation of the situation, the plate selection and prebending can be completed before starting the surgery, and open reduction can be guided by the curvature of the plate. Another advantage of pre-selecting a plate is that only the targeted surface of the bone has to be prepared, which limits the damage to surrounding tissue.

Also instead of using k-wires, the surgeon can use the plate to reposition and reconstruct the bone. This is possible when one side of the fractured bone is first attached to the plate and subsequently the other section of the bone is fixated to the plate, as planned preoperatively.

In this case it has been shown that it is possible to obtain an anatomical model for fitting plates and surgical preparation. No intervention of an expensive third party for 3D printing is required. Additionally, the costs of the material are less than 1 euro per clavicle after a relatively small investment of 1700 euro for the 3D printer (figure 3). When properly applied, this method could reduce the incision time and its variability, improve the surgeons workflow and might even reduce the need of removing the plate at a later stage. This method is not confined to clavicles, but is applicable to a broad range of complex fractures.

A.4 Conclusion

Through a pilot study it is shown that, with a low-budget 3D printer and without intervention of a third party, an anatomical plastic model can be created to aid in a surgical intervention in short time. A clinical study is pending for further validation of the method and clinical value.

A.5 References

1. Althausen PL, Shannon S, Lu M, OMara TJ, Bray TJ. Clinical and financial comparison of operative and nonoperative treatment of displaced clavicle fractures. J Shoulder Elbow Surg 2013;22:608-11. doi: 10.1016/j.jse.2012.06.006

2. Bagaria V, Deshpande S, Rasalkar DD, Kuthe A, Paunipagar BK. Use of rapid prototyping and three-dimensional reconstruction modeling in the management of complex fractures, Eur J Radiol. 80 (2011) 814820, ISSN 0720-048X, doi:10.1016/j.ejrad.2010.10.007.

3 Brown GA, Firoozbakhsh K, DeCoster TA, Reyna JR Jr, Moneim M. Rapid prototyping: the future of trauma surgery? J Bone Joint Surg Am 2003;85(Suppl 4):49-55

4. Chung KJ, Hong do Y, Kim YT, Yang I, Park YW, Kim HN. Preshaping plates for minimally invasive fixation of calcaneal fractures using a real-size 3D-printed model as a preoperative and intraoperative tool. Foot Ankle Int. 2014 Nov;35(11):1231-6. doi:10.1177/1071100714544522

5. Cunningham BP, McLaren A, Richardson M, McLemore R. Clavicular length: the assumption of symmetry. Orthopedics. 2013; 36(3):e343-e347. doi:10.3928/01477447-20130222-24

6. Frame M, Huntley JS. The Scientific World Journal 2012, Article ID 838575, 7 pages. doi:10.1100/2012/838575

7. Jeong HS, Park KJ, Kil KM, Chong S, Eun HJ, Lee TS, et al. Minimally invasive plate osteosynthesis using 3D printing for shaft fractures of clavicles: technical note. Arch Orthop Trauma Surg. 2014 Nov;134(11):1551-5. doi:10.1007/s00402-014-2075-8

8. Marsh JL, Slongo TF, Agel J, Broderick JS, Creevey W, DeCoster TA, et al. Fracture and dislocation classification compendium - 2007: Orthopaedic Trauma Association classification, database and outcomes committee. J Ortho Trauma 2007;21. S72-74. PMID:18277234

9. Melenevsky Y, Yablon CM, RamappaA, Hochman MG. Clavicle and acromioclavicular joint injuries: a review of imaging, treatment, and complications. J Skeletal Radiology 2011; 40:831842. doi:10.1007/s00256-010-0968-3
10. Postacchini F, Gumina S, De Santis P, Albo F. Epidemiology of clavicle fractures. J Shoulder Elbow Surg 2002;11:452-6. doi:10.1067/ mse.2002.126613
11. Rengier F, Mehndiratta A, von Tengg-Kobligh H, Zechmann CM, Unterhinninghofen R, Kauczor HU, et al. 3D printing base on imaging data: review of medical applications. Int J Comput Assist Radiol Surg 2010;5:335-41. doi:10.1007/s11548-010-0476-x
12. van der Meijden OA, Gaskill TR, Millett PJ. Treatment of clavicle fractures: current concepts review. J Shoulder Elbow Surg 2012;21: 423-9. doi:10.1016/j.jse.2011.08.053
13. Virtanen K, Remes V, Malmivaara A, Paavola M. Treatment of clavicle fractures: systematic review. Suomen Ortopedia ja Traumatologia 2009;32:134-9.
14. Wijdicks FJ, Houwert RM, Millett PJ, Verleisdonk EJ, Van der Meijden OA. Systematic review of complications after intramedullary fixation for displaced midshaft clavicle fractures. Can J Surg 2013;56:58-64. doi:10.1503/cjs.029511

A.6 Figures and Table legends

Figure 1: Plastic replica of the pseudarthrosis of the fractured right clavicle (bottom) and mirrored contralateral, left and healthy, clavicle (top). Around the fracture the callus formation can be seen. During surgery the callus was removed.

Figure 2: 3D mesh models of the fractured clavicle (bottom) and the mirrored contralateral clavicle (top).

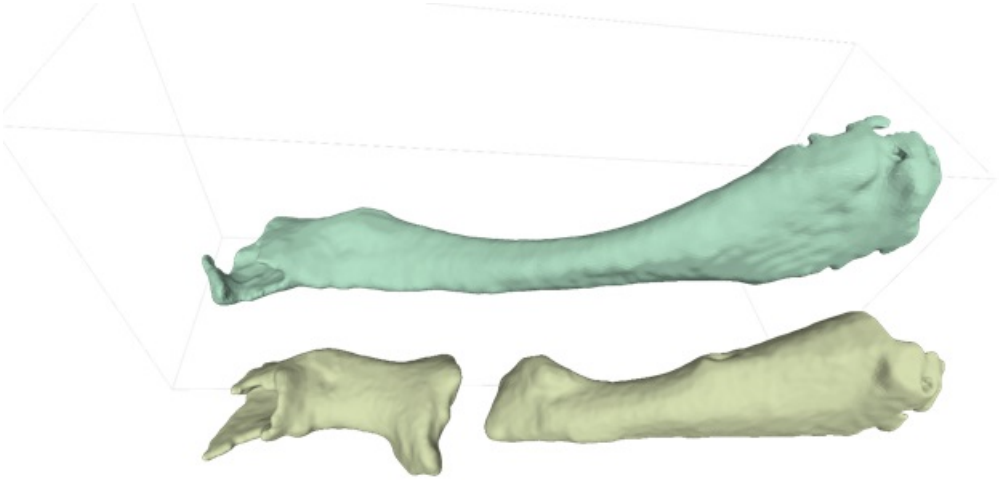

Figure 3: Low budget 3D printer, BQ Witbox. Uses the technique Fused deposition modeling.

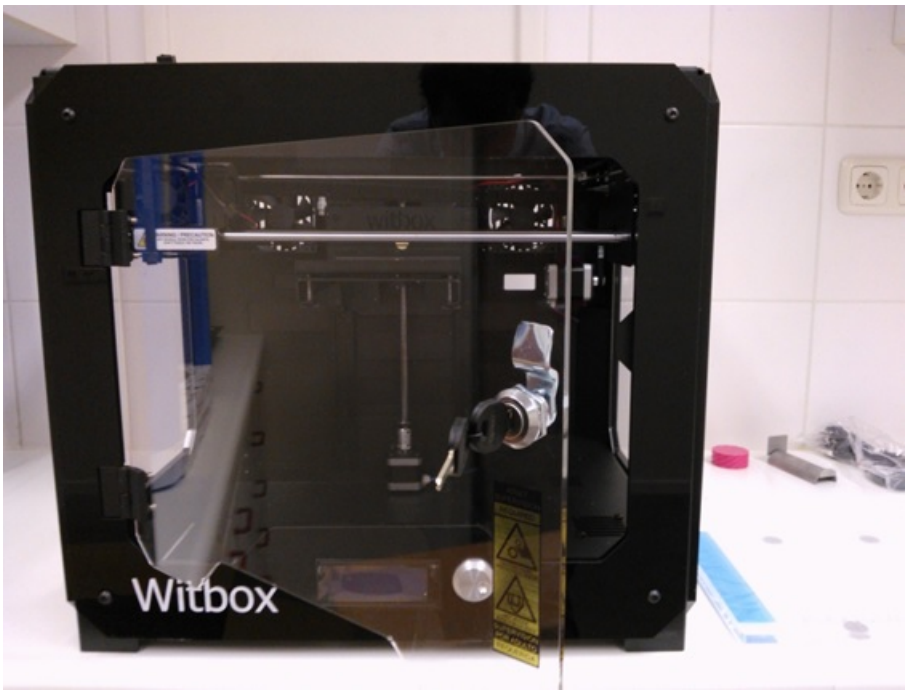

Figure 4: The osteosynthetic plate after bending it to the curvature of the mirrored contralateral model. The plate is outlined on the plastic model.

Figure 5: X-Ray image of the clavicle. A) 5 days prior to and B) 64 day after surgery

Appendix B

Literature overview

Table B.1: Overview of literature concerning Rapid prototyping in orthopaedics and trauma.

Study	Country/year	Department	Pathology	Application	Main findings
Ahn et al.	Korea/2006	Orthopaedics, Medical engineering	Distal tibia, Pelvic wing	Planning, OS material selection	Efficient surgical tool
Chung et al.	Korea/2014	Orthopaedics	Calcaneus	Planning, plate bending.	Positive
Jeong et al.	Korea /2014	Orthopaedics	Clavicle	Plate bending, MIPO	Improved accuracy, minimal invasive.
Bagaria et al.	India/2010	Orthopaedics	Spine, acetabulum, calcaneus, proximal femur	Planning screw trajectory, and prebending plates	Time reduction, near anatomical reduction.
Yang et al.	China/2011	Orthopaedics	Thoracic spine deformity	Planning with navigation template	Beneficial for planning, improved accuracy, efficacy and safety
Qioa et al.	China/2015	Orthopaedics	Radius malunion	Osteotomy with 3D printed external fixator	Improved accuracy, minimal invasive, easy fracture manipulation
Brown et al.	Mexico/2003	Orthopaedics	Overview	Overview of possibilities	The future of trauma surgery.
Starosolsky et al.	USA/2013	Peadiatrics, orthopaedics	pediatric musculoskeletal disorders	Inform parents and patients	Improved understanding in anatomy and pathology
Watson et al.	USA/2014	Surgery	Hepatic vein model	Resident education	Inexpensive and save
Olson et al	Canada/2014	Orthopaedics	Hip joint	Resurfacing with saw/drill guids	Improved accuracy
Biglino et al.	UK/2011	Cardiovascular Imaging	Cardiac, orthopaedic, maxillofacial	Planning, eg stent placement	Good clinical assessment, measurments and quick and instinctive understanding of morphology.
Frame et al.	UK/2012	Orthopaedics	Antebrachi fracture	Guide to apply rapid prototyping	Simple, cost effective for complex fracture patterns with tissue coverage.
Rengiers et al.	Germany/ 2010	Radiology	Overview of application	Overview	Feasible for surgical and prosthetic applications.

Appendix C

Pseudo algorithm Matlab scrip

Here is the Matlabscript of the program explaned in pseudocode. Pseudocode is an informal description of the script and with some explenation is given about the used techniques. This appendix is added to supply a better understanding in the program and is a section from the respective M2 internship report, as it is develloped in this intership. Minor adjustments were made for this thesis and the relevant adjustments come forward in the main tekst. A video of the program is included in chapter 3 section ”Virtual processing” as figure 3.1.2.

1. **Load the CT scan**

   Select within the CT the file named “series for 3D”, by clicking “load CT” and, after selecting “DICOM”, browse in the pop up to the folder where the DICOM files are stored, probably on the disk, and select one file. The script will extract the series. If it is not clear which folder corresponds with which needed series, it is possible to use the DICOM viewer on the CD to find the right one, they are listed in the same order.

   When loading a DICOM file, the script automatically creates a folder within the current Matlab folder, named “Data” if it does not already exist. Within Data a folder will be created and named after the birthdate of the subject. Be aware of this when subjects have the same birthdates to avoid an overwrite. Here the scan will be stored as a Matlab file (named CT.mat) again in a folder named after the series.

   If a scan needs to be loaded for a second time, the faster option is to click “Matlab file” instead of “Dicom”, and select the file created when the series are loaded from the disk the first time.

2. **Select the region of interest**

   After a moment the series are loaded and a coronal overview image will pop up. Within this image two vertices need to be selected to mark the opposite corners of the frame around the targeted clavicle. Hereafter another image will pop up to select the vertices of the framework for the last dimension, the upper and lower limit. When finished the series are displayed to control the framework, click “Auto W/L” if the images are not visible. This is the moment to check if the entire clavicle is present. After closing the figure this fact needs to be confirmed, if not the case the selection of the region of interest will start over.

   The program cuts of the pixels and slices outside the region of interest/framework and creates new data set centred at the clavicle.

3. **Filtering**

   Before continuing to the segmentation it is possible to choose if filtering is necessary. Filtering will take some extra time, but can proof its worth when the scan contains troublesome noise. The filter is constructed as a Gaussian in three dimensions with a diameter of 5 pixels.

4. **Segmentation**

   Segmentation consists of a relatively simple thresholding and post-processing. Default threshold is set at 1250 but can be easily altered in the editbox underneath the button “Apply threshold”. By clicking this button the segmentation starts with setting a threshold and the results will be displayed. Check these results for the clavicle visualised as desired.

   In a step further in the program the clavicle will be separated from the other bone structures. To do so no pixels must connect the clavicle with the other structures. So if possible check the results on connecting pixels, and when this is the case, increase the threshold in the editbox and click again on the button “Apply threshold”.

   The program takes all the pixel values in the scan above the threshold and sets those to one, while the rest is set to null. Then the pixels with value one are eroded and dilated, with as a structural

element matrix of 3x3x3. This means that around the volume of ones the edge with thickness of one pixel is removed and then again added. The purpose of eroding and dilating is removing single pixels, which are considered noise.

5. **Differentiate the clavicle**

   With the segmentation all the object with a pixel value above the threshold are set to one, as explained at the end of the previous step. Of those object only the clavicle is needed. After the button “Select clavicula” is clicked upon, the object with the most pixels will be shown. And when the figure is closed, the question “Was this piece (part of) the clavicle?”. So before closing the figure, check the entire scan for the clavicle. When the question is asked click yes or no respectively, or click finish if it is assumed that no more parts are left. After answering the question the second biggest object is shown then the third, and so on. If besides the clavicle also another structure is shown, than there are connecting pixels between these objects and are considered as one object. This happens when the threshold was set to low. If this happens, click “finish”, and return to the previous step: Segmentation.

   Following this selection the program will fill the holes, or marrow, for a solid bone object.

6. **Create the surface model of the clavicle**

   The next step is converting the objects consisting of ones into a surface model made up of vertices and faces, by clicking on the button “Create model”. The model well be rendered and shown in the program and is able to be rotated. The vertices are scaled to the pixel dimensions to create a clavicle with the same dimensions as the original.

7. **Save model in .STL extension**

   For further processing of the model outside Matlab, the model has to be converted to a .stl file, which happens when clicked on “save model”. The program will ask how the file should be named and if its the left or right clavicle.

8. **Done**

   When done and content, close the GUI.

The created model is loaded in Meshlab to clean the .stl file from non manifold vertices and faces. After cleaning, fragments can be separated and saved as different .stl files, to be able to print them separately and more efficient. Separation is done by removing al the vertices and faces not belonging to the fragment and filling the hole left in the surface afterwards.
At last the modelled fragments are loaded in Cura. Cura adds a support structure under the model to prevent it from falling during the process. It is recommended to rotate the models that the use of support structure is at a minimum, but still stands firm. Keep the highest point as low as possible as this saves time. When all fragments are placed to content, printing can finally start.

Appendix D

CT protocol

Table D.1: List of settings in the CT protocol.

Parameter:	Value
Scanlength:	100 mm
Reconstruction diameter:	$<$500 mm
Matrix size:	1024 x 1024
Dose (DLP) :	100 mGy 20
Equivalent dose:	1 mSv
Slice-thickness:	0.9 mm
Increment:	0.45 mm
Collimation:	64x0.625 mm
Pitch:	0.392
Rotation time:	0.75 seconds

Appendix E

Specifications Witbox Bq 3D printer

bq

bq WITBOX

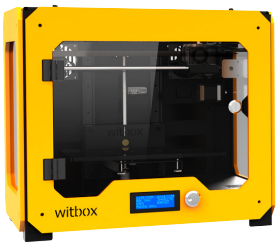

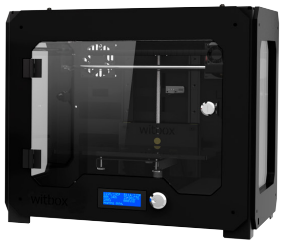

TECHNICAL SPECIFICATIONS

Dimensions

Dimensions: (x)*505 x (y)388 x (z)450 mm*
Work area: (x)297 x (y)210 x (z)200 mm
Dimensions (box): (x)643 x (y)547 x (z)647 mm
Weight: 28 kg

Layer Resolution

Very high: 60 microns
High: 100 microns
Medium: 200 microns
Low: 300 microns

Print time

Recommended speed: 60 mm/s
Maximum recommended: 80 mm/s

Electronics

Ramps 1.4
Mega 2560
LCD screen with rotary encoder and push-button navigation
348W power source
100k thermistors in the extruder
40W, 12V heater cartridge

General Mechanics

Powder-coated steel chassis
Toughened chrome bars for carriages X, Y and Z
Igus bearings for X, Y and Z
Igus cable-chains
Igus power screw for the Z axis with flexible motor coupling
Powder-coated moving parts and supports
Glass base (8 mm thick)
Three-point printer base levelling system with damping
Quick-change printer base system with neodymium magnets

Extruder Mechanics

Single extruder
Own-design extruder
0.4 mm nozzles
Cooling system for parts

Software

Open Source

Connectivity

Standard SDHC card reader with 4 GB card included
USB port type B

Safety

Enclosed machine with locking safety door

Materials

PLA 1.75 mm

More info

Stackable
Rear feeder system based on the Fibonacci spiral[1]

Box content

1 PLA spool
4 GB SD card
Tools for replacing the hot end
Spooler
Printed test part
1 replacement hot end
2 needles for extruder maintenance
Witbox feet
Glass base
Calibration template
Spatula
Wire brush
Power cable
USB cable
Set of two keys
2 side panels and 1 top panel

EAN: 8436545512418 - P/N: 04BQWIT01
EAN: 8436545512425 - P/N: 04BQWIT02
EAN: 8436545512432 - P/N: 04BQWIT03

8 436545 512432 8 436545 512418 8 436545 512425

CE

** The device image isn't contractual*

[1] Patent pending

Appendix F

Setting Cura

Table F.1: List of settings in the Cura 3D printing sofware.

Quality	
Layer height (mm)	:0.3
Shell thickness (mm)	:0.8
Enable retraction	:Yes
Fill	
Bottom/Top Thickness (mm)	:0.9
Fill Density (%)	:10-15
Speed and Temperature	
Print speed (mm/s)	:60 - 80
Printing temperature	:215
Support	
Support type:	*Everywhere*
Stucture type	:Grid
Overhang angle for support (deg)	:60
Fill amount (%)	:5-10
Distance X/Y (mm)	:0.7
Distance Z(mm)	:0.2
Platform adhesion type:	*Raft*
Extra margin (mm)	:3
Line Spacing (mm)	:2
Base thickness (mm)	:0.3
Base line width (mm)	:0.7
Interface thickness (mm)	:0.2
Interface line width (mm)	:0.2
Airgap	:0.0
First Layer Airgap	:0.22
Surface layers	:1
Surface layer thickness (mm)	:0.27
Surface layer line width (mm)	:0.4

Table F.2: List of settings in the Cura 3D printing sofware. (Continuation)

Filament	
Diameter (mm)	:1.75
Flow (%)	:100.0
Machine	
Nozzle size (mm)	:0.4
Retraction	
Speed (mm/s)	:40
Distance (mm)	:4
Quality	
Initial layer thickness (mm)	:0.3
Initial layer line width (%)	:120
Cut off object bottom (mm)	:0
Speed	
Travel speed (mm/s)	:130
Bottom layer speed (mm/s)	:20
Cool	
Minimal layer time (sec)	:5
Enable cooling fan	:yes

Appendix G

Case descriptions intervention group

Summary of errors and achievements per case.

Case 1 For preoperative bending the assumption was made that surgical bending pliers would suffice. Also the fitting plates were superior plates and the actual used clavicle plates were superior anterior plates, that had a standard torsion from superior lateral to anterior medial. With solely pliers these (counter)clockwise torsion could not be adjusted. Therefore, the superior anterior torsion did not contribute well in this case and the correct position could not be found perioperatively and had to be bent. In this experience was learned that bending irons were also required in the preoperative setting.

Case 2 The surgery almost dropped from the schedule. Fortunately, two assistants could do the surgery around 6 pm. However, because it was this late, the leading surgeon was not open for input from the researcher who made the preoperative planning. This resulted in an improvised reduction, deviation from the plan and thus an incorrect positioning. This experience learned that the planner, this case the researcher, should get the chance to evaluate and comment on the position of the plate during decision making. Even more important, the leading surgeon should trust the planner. If in one step there is a deviation from the plan the rest becomes useless, as plate shape and screw lengths.

Case 3 This case was originally planned close to case two. Only one sterilization net was available for the trail so preferably 24 hours between surgeries is desired and with haste 11 hours to have the next plate on time. Unfortunately, this case dropped of the schedule and on the day of surgery the trauma was already 30 days old, resulting in a lot of callus formation and therefore a difficult preparation of the bone.

Case 4 As in case 2 the plate was planned to slide over a k-wire used for stabilizing the reduction. This technique is not feasible. Instead a screw was placed under the plate and the plate was bent in an angle to fit over the screw accordingly. The lesson learned from this case was that the locations the instruments used for the temporal reduction should be considered in planning the position of the plate during preoperatively bending.

Case 5 This case the surgeon really took the time to prepare for the surgery in collaboration with the planner, listened to what area of the bone was to be prepared for plate contact and trusted the planners advice on plate positioning as the plate initially did not fit. Lesson here was that trust, good initial bone preparation and taking the time for plate positioning pays off. The result was that all the screw lengths were correct.

Case 6 A lot of callus formation was present. Due to the preparation the alignment was acceptable without extensive bone preparation. To avoid undoing the current healing process, the minimal effort in reduction was accepted and the plate was placed. The plate fitted acceptably, but because no anatomical reduction was aspired. This resulted that the plate did not fit perfectly as well as the screws with a mean deviation of 2 mm.

Case 7 This case was more complex than case 5, however, resulted in a resembling result in both workflow and outcome.

In both groups one subject had the plated removed, coincidental the only women in the study. The subject in the control group had it removed due to irritation of the material and the one in the intervention group because of non-union and infection around the material. The rest of the subjects were happy with the results.

Appendix H

Signed sterilisation protocol

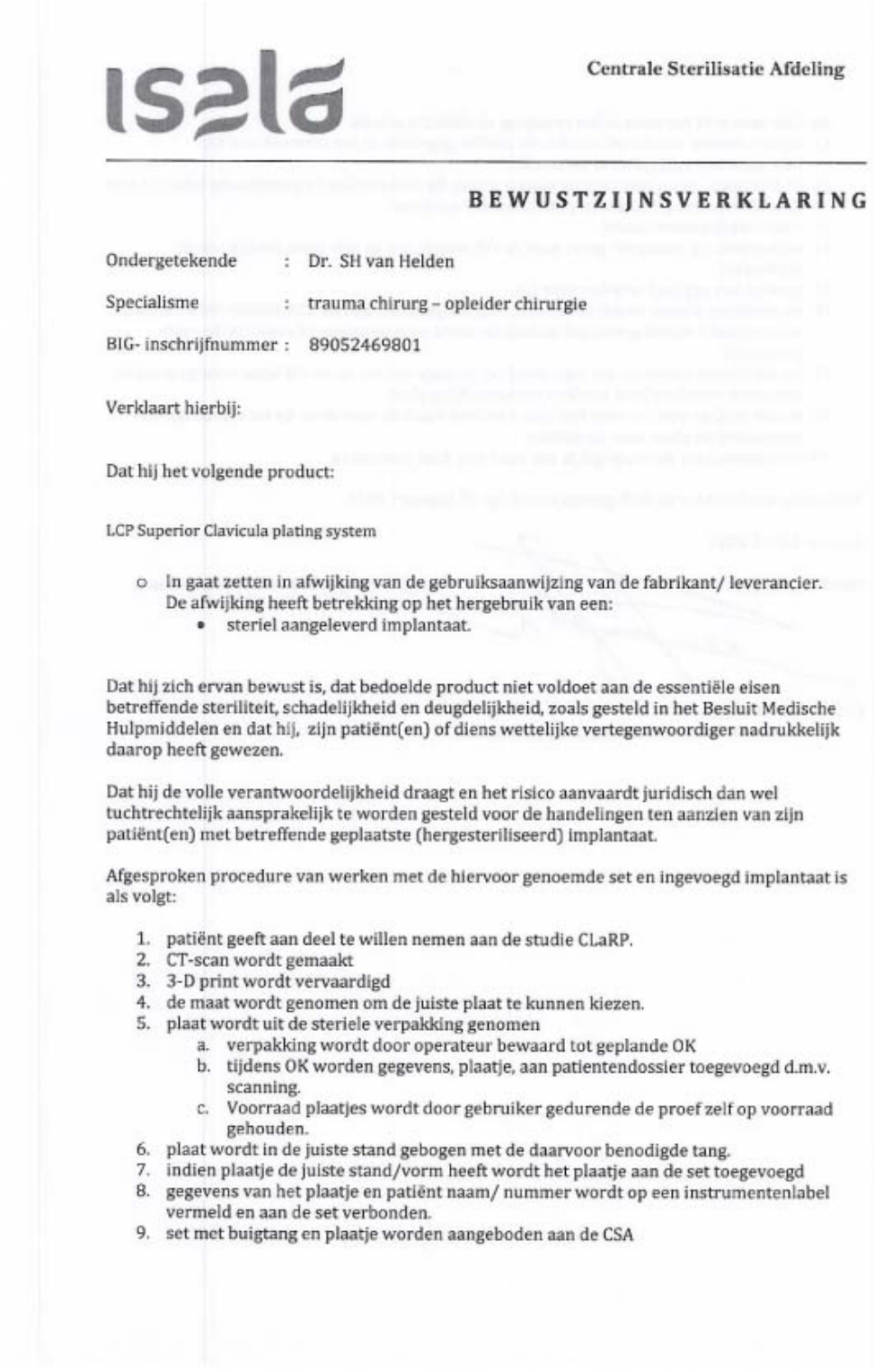

Centrale Sterilisatie Afdeling

BEWUSTZIJNSVERKLARING

Ondergetekende : Dr. SH van Helden

Specialisme : trauma chirurg – opleider chirurgie

BIG- inschrijfnummer : 89052469801

Verklaart hierbij:

Dat hij het volgende product:

LCP Superior Clavicula plating system

- In gaat zetten in afwijking van de gebruiksaanwijzing van de fabrikant/ leverancier. De afwijking heeft betrekking op het hergebruik van een:
  - steriel aangeleverd implantaat.

Dat hij zich ervan bewust is, dat bedoelde product niet voldoet aan de essentiële eisen betreffende steriliteit, schadelijkheid en deugdelijkheid, zoals gesteld in het Besluit Medische Hulpmiddelen en dat hij, zijn patiënt(en) of diens wettelijke vertegenwoordiger nadrukkelijk daarop heeft gewezen.

Dat hij de volle verantwoordelijkheid draagt en het risico aanvaardt juridisch dan wel tuchtrechtelijk aansprakelijk te worden gesteld voor de handelingen ten aanzien van zijn patiënt(en) met betreffende geplaatste (hergesteriliseerd) implantaat.

Afgesproken procedure van werken met de hiervoor genoemde set en ingevoegd implantaat is als volgt:

1. patiënt geeft aan deel te willen nemen aan de studie CLaRP.
2. CT-scan wordt gemaakt
3. 3-D print wordt vervaardigd
4. de maat wordt genomen om de juiste plaat te kunnen kiezen.
5. plaat wordt uit de steriele verpakking genomen
   a. verpakking wordt door operateur bewaard tot geplande OK
   b. tijdens OK worden gegevens, plaatje, aan patientendossier toegevoegd d.m.v. scanning.
   c. Voorraad plaatjes wordt door gebruiker gedurende de proef zelf op voorraad gehouden.
6. plaat wordt in de juiste stand gebogen met de daarvoor benodigde tang.
7. indien plaatje de juiste stand/vorm heeft wordt het plaatje aan de set toegevoegd
8. gegevens van het plaatje en patiënt naam/ nummer wordt op een instrumentenlabel vermeld en aan de set verbonden.
9. set met buigtang en plaatje worden aangeboden aan de CSA

10. CSA verwerkt het setje in het reiniging, desinfectie proces.
11. bij de controle van de set worden de patiënt gegevens in het tekstvak van het instrumenten volgsysteem verwerkt.
12. CSA verpakt de set met tang en plaatje draait de desbetreffende identificatie label uit met daarop vermeld set naam en patiënt naam/ nummer.
13. setje wordt gesteriliseerd
14. setje wordt op transport gezet naar de OK alwaar het op zijn vaste locatie wordt ingeruimd
15. patiënt kan gepland worden voor OK.
16. na plaatsing plaatje wordt de set met tang aangeboden aan de CSA alwaar de set zonder nieuw plaatje wordt gereinigd, gedesinfecteerd en gesteriliseerd conform de vaste procedure.
17. na sterilisatie wordt de set ingeruimd op de vaste locatie op de OK klaar voor gebruik bij een acute inzetbaarheid zonder voorbewerking plaat.
18. indien nieuwe patiënt voor test zich aandient haalt de operateur de set van de OK en prepareert de plaat voor de patiënt.
19. vervolgens gaat de route gelijk aan start van deze procedure.

Test/onderzoek is door de RvB goedgekeurd op: 17 februari 2015.

Datum: 20-02-2015

Handtekening arts: Handtekening DSMH: (instemming procedure)

C.c; Directie Isala
Inspectie Gezondheidszorg (IGZ) indien gewenst.

Appendix I

Radiations densities of different materials

Table I.1: Overview of the measured Hounsfield units of different materials with their density when known. 734 and 732 are the Dow Corning values of the silicones.

Material /HU	Max	Min	Mean	density
Glass fibre	2248	1042	1589.6	?
PTFE	1066.3	789	945.3	2.18
PVC	1124	770	955.4	1.55
PVDF	799	512	635.7	1.78
Adheseal	880	216	705.4	1.38
POM	467	244	353.6	1.42
Tufnol	336	158	249.1	?
734 (boxed)	180	105	149	1.03
732 (loose)	248	103	171.3	1.04
water	38	-77	-20.2	1
air	-887	-1000	-977	

Figure I.1: Slice of the CT scan from which the Hounsfield units are determined.

Appendix J

Extracurricular cases

J.1 Humerus

In this case an inter-articular fracture of a proximal humerus needed to be fixed. A plastic replica of the anatomy was fabricated. In planning the approach the reduction was based on this replica together with an approximate selection of the osteosyntesis material could be hypothesised. No unsterile versions of the material was available for manual testing preoperatively.

In figure J.1 the shaft and two fragments can be distinguished also with the volume ray casting rendering technique the cortex quality could be assessed to determine what part was optimal for screw placement. No objective measurements were performed, though the surgeon was content with the extra insight.

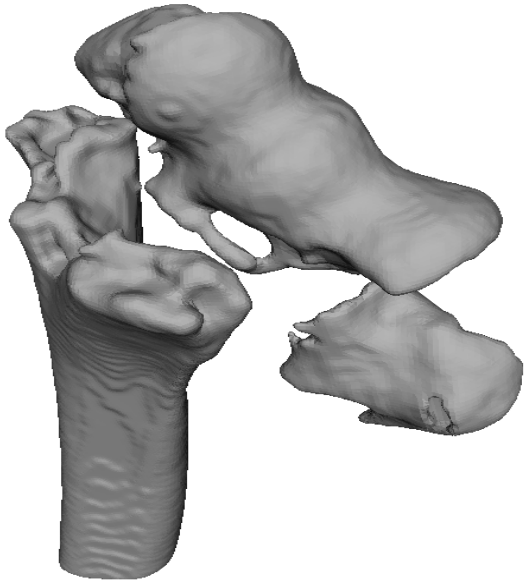

Figure J.1: The 3D model of the distal humerus fracture.

J.2 Pelvis

The pelvic fracture in this was relatively old and for plan of approach a plastic model was requested on real size of the part where the fracture was situated, figure J.2. Unfortunately, when it eventually came down to surgery the plastic model was ignored in plan of approach. Two screws were placed, both incorrect. The first went through the soft tissue ventrally of the pelvis and the second penetrated the sacrum and touched the myelum. The latter cause discomfort and had to be removed through revision surgery a week later to reverse the complications.

J.3 Radius

In this case a fourteen year old boy fractured his forearm and over time a developed a malunion of the radius. This means that the fracture is healed, however the two main fragments jointed non-anatomical.

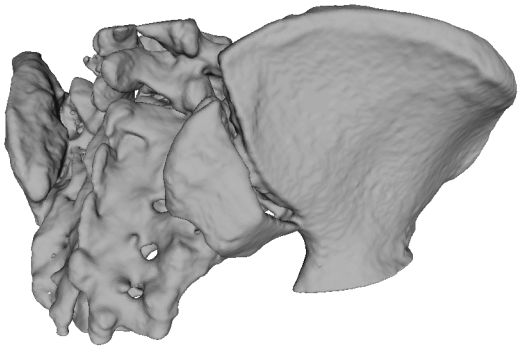

Figure J.2: The 3D model of the pelvic fracture.

This malunion caused a supination error which could be corrected with an osteotomy. For preparation purposes and informing the patient, the fractured radius and the mirrored healthy radius, as reconstruction, was 3D printed in real size, see 3D models in figure J.3. Additionally prior to surgery the rotation error was calculated from using the two models. The proximal ends of the two models were virtually aligned and subsequently the malunion distal end was aligned over the healthy mirrored distal end, figure J.4 for alignment of the proximal end. From the resulting transformation matrix the axis angle representation could be calculated. The plane perpendicular to the axis could be interpreted as the saw plane and the angle the rotation correction, 62.29 degrees . Unfortunately, no instruments were present for such accurate osteotomy. Right in figure J.5 the surgical intervention is shown with K-wires for rotation and a triangle to test the 60 degrees rotation error. Similar method and surgical templates are researched in the Amsterdam Medical Centre (AMC) [17, 18].

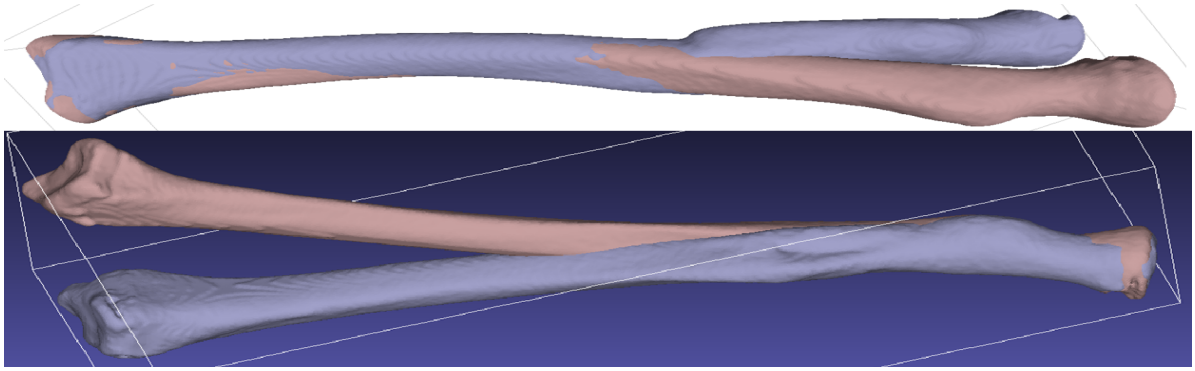

Figure J.3: Poster image: The 3D model of the radius malunion. In the top image the distal ends are aligned and in the bottom image the proximal ends are aligned. 3Dmodel: The 3D model of the radius malunion next to the mirrored healthy contralateral radius.

Figure J.4: The 3D model of de radius malunion aligned the mirrored healthy contralateral radius at the proximal end.

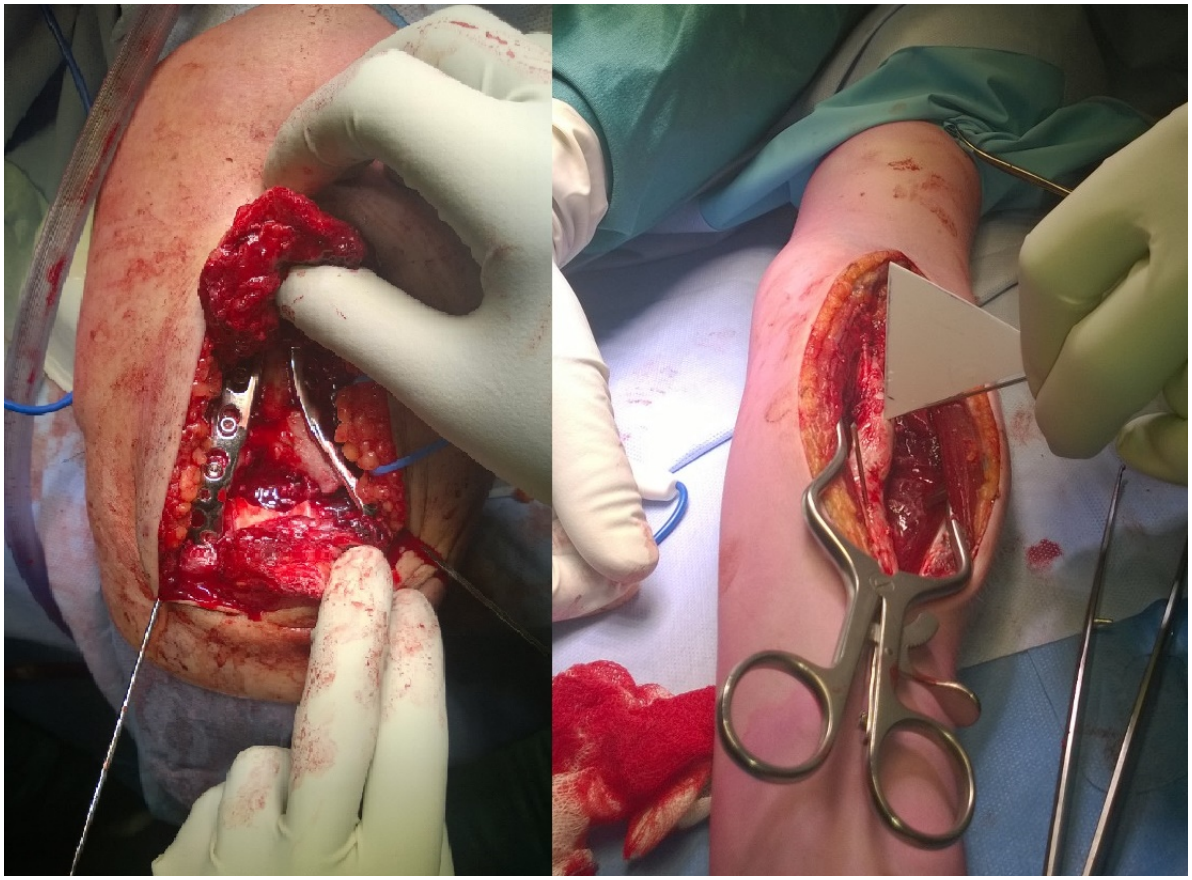

Figure J.5: The surgical interventions of left the humerus case with osteosynthesis material and right the radius case with improvised triangle to accommodate for the 60 degrees rotation.